



1 **Measurement report: Source apportionment of carbonaceous aerosol using**
2 **dual-carbon isotopes (^{13}C and ^{14}C) and levoglucosan in three northern Chinese**
3 **cities during 2018–2019**

4

5 Huiyizhe Zhao ^{a, c, d}, Zhenchuan Niu ^{a, b, c, d, e, *}, Weijian Zhou ^{a, b, c, d, *}, Sen Wang^f, Xue
6 Feng^g, Shugang Wu ^{a, c}, Xuefeng Lu ^{a, c}, Hua Du ^{a, c},

7 ^a *State Key Laboratory of Loess and Quaternary Geology, CAS Center for Excellence*
8 *in Quaternary Science and Global Change, Institute of Earth Environment, Chinese*
9 *Academy of Sciences, Xi'an 710061, China*

10 ^b *Open Studio for Oceanic-Continental Climate and Environment Changes, Pilot*
11 *National Laboratory for Marine Science and Technology (Qingdao), Qingdao 266061,*
12 *China*

13 ^c *Shaanxi Provincial Key Laboratory of Accelerator Mass Spectrometry Technology*
14 *and Application, Joint Xi'an AMS Center between IEECAS and Xi'an Jiaotong*
15 *University, Xi'an 710061, China*

16 ^d *University of Chinese Academy of Sciences, Beijing 100049, China*

17 ^e *Shaanxi Guanzhong Plain Ecological Environment Change and Comprehensive*
18 *Treatment National Observation and Research Station, Xi'an, China*

19 ^f *Shaanxi Key Laboratory of Earth Surface System and Environmental Carrying*
20 *Capacity, College of Urban and Environmental Sciences, Northwest University, Xi'an,*
21 *China*

22 ^g *Xi'an Institute for Innovative Earth Environment Research, Xi'an, China*

23 **Correspondence:** Zhenchuan Niu (niuzc@ieecas.cn) and Weijian Zhou
24 (weijian@loess.llqg.ac.cn)

25



26 **Abstract**

27 In this study, we investigated the characteristics and changes in the sources of
28 carbonaceous aerosols in northern Chinese cities after the implementation of the
29 Action Plan for Air Pollution Prevention and Control in 2013. We collected PM_{2.5}
30 samples from three representative inland cities, viz. Beijing (BJ), Xi'an (XA), and
31 Linfen (LF) from January 2018 to April 2019. Elemental carbon (EC), organic carbon
32 (OC), levoglucosan, stable carbon, and radiocarbon were measured in PM_{2.5} to
33 quantify the sources of carbonaceous aerosol employing Latin hypercube sampling.
34 The best estimate of source apportionment showed that the emissions from liquid
35 fossil fuels contributed $33.6 \pm 12.9\%$, $26.6 \pm 16.4\%$, and $24.6 \pm 13.4\%$ of the total
36 carbon (TC) in BJ, XA, and LF, whereas coal combustion contributed $11.2 \pm 9.1\%$,
37 $19.2 \pm 12.3\%$, and $39.2 \pm 20.5\%$, respectively. Non-fossil sources accounted for $55 \pm$
38 11% , $54 \pm 10\%$, and $36 \pm 14\%$ of the TC in BJ, XA, and LF, respectively. In XA,
39 $48.34 \pm 32.01\%$ of non-fossil sources was attributed to biomass burning. The highest
40 contributors to OC in LF and XA were fossil sources ($65.4 \pm 14.9\%$ and $44.9 \pm 9.5\%$,
41 respectively), whereas that in BJ was non-fossil sources in BJ ($56.1 \pm 16.7\%$). The
42 main contributors to EC were fossil sources, accounting for $92.9 \pm 6.13\%$, $69.9 \pm$
43 20.9% , and $90.8 \pm 9.9\%$ of the total EC in BJ, XA, and LF, respectively. The decline
44 (6–17%) in fossil source contributions in BJ and XA since the implementation of the
45 Action Plan indicates the effectiveness of air quality management. We suggest that
46 measures targeted to each city should be strengthened in the future.

47

48 **Keywords:** carbonaceous aerosols; radiocarbon; stable carbon; biomass; fossil fuel;
49 source apportionment

50



51 **1 Introduction**

52 Atmospheric aerosols are extremely complex suspension systems. Carbonaceous
53 aerosols are an important component of atmospheric aerosols, accounting for
54 approximately 10–60% of the total mass of global fine particulate matter (Cao et al.,
55 2003, 2007; Feng et al., 2009). Carbonaceous aerosols contain elemental carbon (EC),
56 organic carbon (OC), and inorganic carbon (IC). IC is mainly derived from sand dust,
57 it has a low concentration and simple composition, and it can be removed via acid
58 treatment (Clarke et al., 1992). EC is produced by incomplete combustion and is
59 directly discharged from pollution sources. It can cause global warming by changing
60 the radiative forcing and ice albedo (Jacobson et al., 2001; Kiehl et al., 2007). OC is a
61 complex mixture of primary and secondary pollutants produced by the combustion of
62 domestic biomass and fossil fuels. It is an important contributor to tropospheric ozone,
63 photochemical smog, and rainwater acidification, and it can significantly impact
64 regional and global environments through biogeochemical cycling (Jacobson et al.,
65 2000; Seinfeld et al., 1998). Therefore, identifying and quantifying the source
66 contributions of carbonaceous aerosols can provide a scientific basis for the
67 management of regional air quality.

68 The natural radiocarbon isotope (^{14}C) can be used to study the source of
69 atmospheric particulate matter and to quantitatively and accurately distinguish the
70 contributions of fossil and non-fossil sources (Clayton et al., 1955; Currie, 2000;
71 Szidat, 2009). In recent decades, this method has been widely used to trace non-fossil
72 carbonaceous aerosols in various regions (Ceburnis et al., 2011; Huang et al., 2010;
73 Lewis et al., 2004; Szidat et al., 2009; Vonwiller et al., 2017; Yang et al., 2005; Yttri et
74 al., 2011; Zhang et al., 2012, 2017). Stable carbon isotope (^{13}C) is useful geochemical
75 marker that can provide valuable information about both the sources and atmospheric



76 processing of carbonaceous aerosols (López-Veneroni, 2009; Widory, 2006), and they
77 have been applied in various types of environmental research to identify emission
78 sources (Cachier et al., 1985, 1986; Cao et al., 2011; Chesselet et al., 1981; Fang et al.,
79 2017; Kawashima & Haneishi, 2012; Kirillova et al., 2013; Liu et al., 2014; Wang et
80 al., 2012). The analysis of $^{13}\text{C}/^{12}\text{C}$ can refine ^{14}C source apportionment because both
81 coal and liquid fossil fuels are depleted of ^{14}C while their ^{13}C source signatures are
82 different (Andersson et al., 2015; Li et al., 2016; Winiger et al., 2017). Levoglucosan
83 (Lev), a thermal degradation product of cellulose combustion, is a common molecular
84 tracer that can be used to evaluate the contribution of biomass burning (Hoffmann et
85 al., 2010; Locker et al., 1988; Simoneit et al., 1999). The combination of the carbon
86 isotope analysis and Lev can further divide the contributions of different
87 carbonaceous sources. Some studies have confirmed the feasibility of this
88 combination (Claeys et al., 2010; Gelencsér et al., 2007; Genberg et al., 2011; Huang
89 et al., 2014; Kumagai et al., 2010; Liu et al., 2013; Niu et al., 2013; Zhang et al.,
90 2015).

91 Cities in northern China have been affected by severe haze for several decades.
92 After the Action Plan for Air Pollution Prevention and Control (hereafter simplified as
93 “Action Plan”) was promulgated in 2013, all parts of China responded to the issue and
94 held numerous air quality management practices (CSC, 2013). In 2020, the average
95 $\text{PM}_{2.5}$ concentration in Chinese cities across the country decreased by 54.2%
96 compared to that in 2013 (MEE, 2014, 2021). In 2020, the proportion of clean energy
97 consumption, such as that of natural gas and electricity, increased by 7.9% compared
98 to that in 2013, and the proportion of coal combustion decreased by 9.7% (NBS,
99 2021). Before the Action Plan, fossil fuel sources were identified as the main
100 contributor to carbonaceous aerosols in Chinese cities (56–81%) (Ni et al., 2018, Niu



101 et al., 2013, Shao et al., 1996; Sun et al., 2012; Yang et al., 2005). In this study, we
102 aimed to determine the main contribution of the current carbonaceous aerosols in
103 northern Chinese cities. Also, we aimed to identify whether changes in energy type
104 and emission control caused a change in the source of carbonaceous aerosols.

105 To address those issues, we conducted a source apportionment of carbonaceous
106 aerosols based on yearly measurements of OC, EC, Lev, ^{13}C , and ^{14}C in $\text{PM}_{2.5}$,
107 combined with Latin hypercube sampling (LHS), in three representative northern
108 Chinese cities during 2018–2019. This study provides a comprehensive understanding
109 of current sources of carbonaceous aerosol after the implementation of the Action
110 Plan in Chinese cities.

111

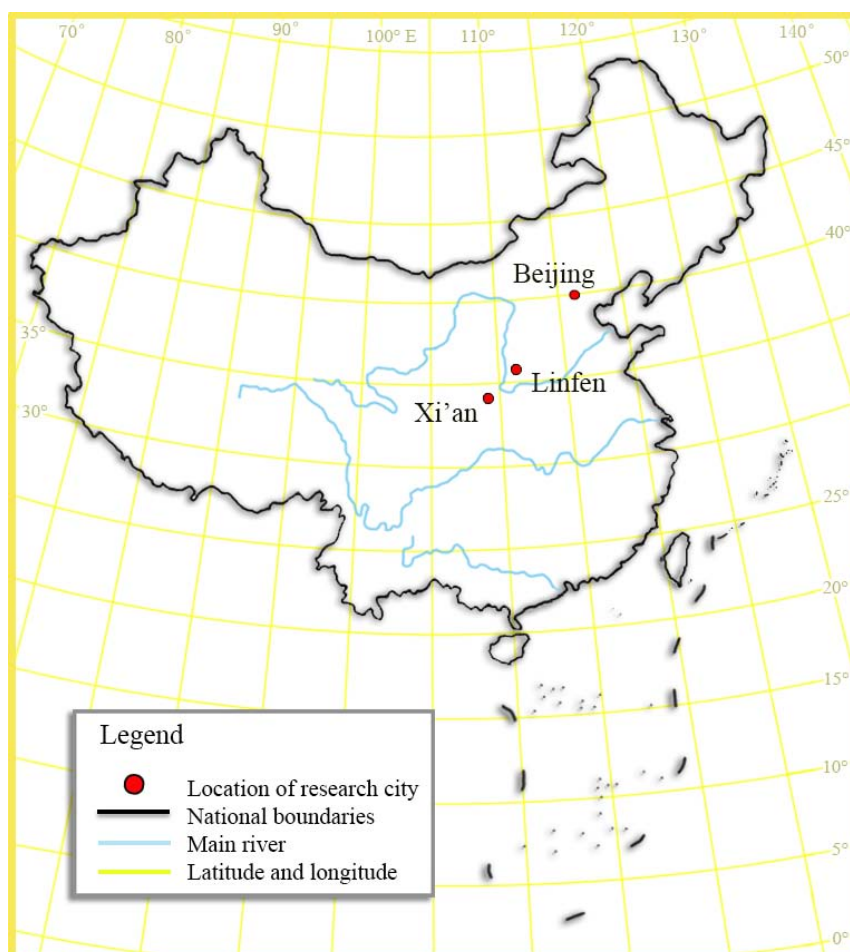
112 **2 Methods**

113 **2.1 Research sites**

114 We selected one urban sampling site in Beijing (BJ), one in Xi'an (XA), and one
115 in Linfen (LF) (Fig. 1). BJ is the capital of China, one of the largest megacities in the
116 world, and the central city of the Beijing–Tianjin–Hebei economic region. It has a
117 population of more than 20 million and has experienced serious air pollution problems
118 in the past few decades. XA, the capital of Shaanxi Province, is the ninth-largest
119 central city and an important city of the Northwest Economic Belt in China. It is
120 located in a basin surrounded by mountains on three sides, where atmospheric
121 pollutants are discharged mainly from the basin and are less affected by other urban
122 areas (Cao et al., 2009; Shen et al., 2011). LF is located in western Shanxi Province
123 and is one of the representative cities in the northern air-polluted region. Shanxi
124 Province is the center of Chinese energy production and chemical metallurgy
125 industries; its coal production and consumption were approximately 736.81 million



126 tons and 349.07 million tons, accounting for 27.05% and 12.42% of the Chinese total
127 in 2019, respectively (NBS, 2020; SPBS, 2020). The air quality in LF was ranked in
128 the worst ten in China from 2018 to 2020 (MEE, 2019, 2020, 2021). According to
129 China Central Television (CCTV) reports, the atmospheric SO_2 concentration in LF
130 exceeded $1000 \mu\text{g m}^{-3}$ several times during January 2017 (CCTV, 2017). XA and LF
131 heavily suffer from air pollution in the Fenwei Plain. In July 2018, the State Council
132 issued the Three-Year Action Plan to Win the Blue Sky Defense War. this included
133 the Fenwei Plain as one of the key areas in which to prevent and control pollution
134 (CSC, 2018).



135



136 Fig. 1 Locations of Beijing (BJ), Xi'an (XA), and Linfen (LF).

137 The first site was located in the northwest of BJ, on the rooftop of the Research
138 Center for Eco-Environmental Sciences, Chinese Academy of Sciences (40°0'33" N,
139 116°20'38" E). The site was approximately 200 m from the road. The second site was
140 located southwest of XA, on the rooftop of the School of Urban and Environmental
141 Sciences in Northwest University (34°15'36" N, 108°88'53" E). Living quarters and
142 teaching areas were located around these two sampling sites. The third site was
143 located in Houma, a county-level city of LF, on the rooftop of a residential building
144 (35°63'56" N, 111°39'53" E). There was no industrial pollution near each site and
145 they were representative urban sites.

146 2.2 Sample collection

147 At BJ and XA, PM_{2.5} samples were collected on the 7th, 14th, 21st, and 28th of
148 each month from April 28, 2018, to April 21, 2019. In LF, seven consecutive days in
149 each season were selected for sample collection, and the sampling periods were
150 concentrated in January, April, July, and October 2018.

151 Samples in each city were collected continuously on pre-baked quartz fiber
152 filters (203 mm × 254 mm, Whatman UK) using a high-volume (1.05 m³ min⁻¹)
153 sampler (TH-1000CII). To remove the existing carbon in the materials, the filter and
154 foil used for wrapping should be baked in a muffle furnace at 375 °C for 5 h before
155 use. After sampling, the filters were folded, wrapped in pre-baked aluminum foil, and
156 stored at -18 °C until analysis. All filters were weighed after equilibrating at 25 ±
157 1 °C and 52 ± 5% humidity for more than 24 h. 124 PM_{2.5} samples and 4 field blanks
158 were obtained in total.

159 2.3 OC and EC analyses

160 Filter pieces of 0.526 cm² were used to measure the OC and EC using a DRI



161 Model 2001 (Thermal/Optical Carbon Analyzer) at the Institute of Earth Environment,
162 Chinese Academy of Sciences. The Interagency Monitoring of Protected Visual
163 Environments (IMPROVE) thermal/optical reflectance protocol must be followed
164 because OC and EC have different oxidation priorities under different temperatures
165 (Cao et al., 2007; Chow & Watson, 2002). OC and EC were defined as OC1 + OC2 +
166 OC3 + OC4 + OP and EC1 + EC2 + EC3 – OP, respectively, in accordance with the
167 IMPROVE protocol (Chow et al., 2004). Sample analysis results were corrected by
168 the average blank and standard sucrose concentrations of OC and EC, respectively.

169 **2.4 Lev analysis**

170 The molecular tracer (Lev) was determined by high-performance anion exchange
171 chromatography with pulsed amperometric detection (HPAEC-PAD) method at the
172 South China Institute of Environmental Science, Ministry of Ecology and
173 Environment. A quartz filter sample (2 cm²) was extracted with 3 ml of deionized
174 water in a prebaked glass bottle under ultrasonic agitation and was subsequently
175 analyzed using a Dionex ICS-3000 system after filtration. The separation requires an
176 equilibrium period, isocratic elution, and gradient elution. (For a specific description,
177 refer to Zhang et al., 2013.) The instrument sample loop was 100 µL and the detection
178 limit of Lev was 1×10⁻⁸ µg ml⁻¹.

179 **2.5 Stable carbon analysis**

180 The ¹³C compositions were determined using a gas isotopic analyzer (Picarro
181 G2131-i) in conjunction with an elemental analyzer (Elemental Combustion System
182 4010) at the Institute of Earth Environment, Chinese Academy of Sciences.
183 Specifically, 0.2–0.4 mgC of sample was placed in a precombusted tin capsule (6×10
184 mm) and the air was removed by squeezing. The samples were tested at 980 °C and
185 650 °C with 70–80 ml min⁻¹ helium as the carrier gas and 20–30 ml min⁻¹ oxygen as



186 the reaction gas. The resulting gas mixture was then collected in Gas Isotopic
187 Analyzer. Urea standard (CAS Number: 57-13-6) was used as standard sample. ^{13}C
188 data are expressed in delta notation with respect to Vienna Pee Dee Belemnite (VPDB)
189 (Coplen, 1996):

$$190 \quad \delta^{13}\text{C} = \left[\frac{^{13}\text{C}/^{12}\text{C}_{\text{Sample}}}{^{13}\text{C}/^{12}\text{C}_{\text{VPDB}}} - 1 \right] \times 1000\text{‰} \quad (1)$$

191 **2.6 Radiocarbon analysis**

192 The ^{14}C samples were prepared and tested in the laboratory of Xi'an accelerator
193 mass spectrometer (AMS) Center. Carbonate must be removed from the filters using
194 hydrochloric acid (1 M) before combustion. The processed sample was packed in a
195 sealed quartz tube with a silver wire and excessive CuO. The solid sample was then
196 combusted at 850 °C for 2.5 h to convert it into gas after the vacuum degree was less
197 than 5×10^{-5} mbar. The gas sample was passed through a liquid nitrogen cold trap
198 (-196 °C) to freeze CO_2 and water vapor, and then passed through an ethanol–liquid
199 nitrogen cold trap (-90 °C) to remove water vapor and purify CO_2 (Turnbull et al.,
200 2007; Zhou et al., 2014). The collected CO_2 was reduced to graphite via a reduction
201 reaction with zinc particles and iron powder as the reductant and catalyst, respectively
202 (Jull, 2007; Slota et al., 1987). The graphite was pressed into an aluminum container
203 and measured using a 3 MV AMS, with a precision of 3‰ (Zhou et al., 2006, 2007).
204 Forty-nine targets were arranged in sequence in the sample fixed wheel, including
205 forty samples, six OX-II standard samples, two anthracite standard samples and one
206 sugar carbon standard sample each time. AMS online $\delta^{13}\text{C}$ of was used for isotope
207 fractionation correction.

208 The ^{14}C results were expressed as a fraction of modern carbon (f_M) (Currie, 2000;
209 Mook & Van Der Plicht, 1999). It defines as the $^{14}\text{C}/^{12}\text{C}$ ratio of the sample related to
210 the isotopic ratio of the reference year 1950 (Stuiver & Polach, 1977):



211 $f_M = (^{14}\text{C}/^{12}\text{C}_{\text{Sample}})/(^{14}\text{C}/^{12}\text{C}_{1950}).$ (2)

212 Non-fossil fractions (f_{nf}) and fossil fractions (f_f) were determined from the f_M
213 values.

214 $f_{\text{nf}} = f_M \times 100\%$ (3)

215 $f_f = (1 - f_M) \times 100\%$ (4)

216 2.7 Source apportionment of total carbon using ^{14}C and ^{13}C

217 To study the contribution of each fossil source to the total carbon (TC), we used
218 the principle of isotopic chemical mass balance to further separate fossil sources into
219 liquid fossil fuels and coal. Since the amount of carbonaceous aerosol produced by
220 natural gas is very low compared to coal and liquid fossil combustion, its contribution
221 was not considered here (Chen et al., 2005; England et al., 2002; Guo et al., 2014;
222 Yan et al., 2010). In this part, ^{13}C and ^{14}C were combined to calculate the
223 contributions of non-fossil, coal, and liquid fossil sources.

224 $f_{\text{nf}} \times \delta^{13}\text{C}_{\text{nf}} + f_{\text{coal}} \times \delta^{13}\text{C}_{\text{coal}} + f_{\text{liq.fossil}} \times \delta^{13}\text{C}_{\text{liq.fossil}} = \delta^{13}\text{C}_{\text{sample}}$ (5)

225 $f_{\text{coal}} + f_{\text{liq.fossil}} = f_f$ (6)

226 $\delta^{13}\text{C}_{\text{sample}}$ is the $\delta^{13}\text{C}$ of the samples at each site; f_{nf} , f_{coal} , and $f_{\text{liq.fossil}}$ represent the
227 proportions of each source; and $\delta^{13}\text{C}_{\text{nf}}$, $\delta^{13}\text{C}_{\text{coal}}$, and $\delta^{13}\text{C}_{\text{liq.fossil}}$ represent $\delta^{13}\text{C}$ from the
228 corresponding sources. The selection of the reference value is described in detail in
229 Section 2.9.

230 2.8 Source apportionment of OC and EC using ^{14}C and Lev

231 The method combines ^{14}C with the concentration of carbon components and a
232 molecular tracer (Lev) to quantify the sources of OC and EC. Carbon was assumed to
233 originate from fossil fuel combustion, biomass burning, and other non-fossil
234 emissions (Gelencsér et al., 2007). The following is a simple calculation method.

235 EC consists of biomass burning (EC_{bb}) and fossil fuel combustion (EC_{ff}).



236 $EC = EC_{ff} + EC_{bb}$ (7)

237 EC_{bb} was calculated based on the Lev concentration and the estimated EC_{bb}/Lev
238 ratio:

239 $EC_{bb} = Lev \times (EC_{bb}/Lev) = Lev \times [(EC/OC)_{bb}/(Lev/OC_{bb})]$ (8)

240 Then, EC_{ff} was calculated by subtraction (Eq. 7).

241 OC consists of OC from biomass burning (OC_{bb}), fossil fuel combustion (OC_{ff}),
242 and other sources (OC_{other}), including primary and secondary biogenic OC and SOC
243 (secondary organic carbon) from non-fossil emissions.

244 $OC = OC_{bb} + OC_{ff} + OC_{other}$ (9)

245 OC_{bb} was calculated based on the Lev concentration and the estimated Lev/OC_{bb}
246 ratio:

247 $OC_{bb} = Lev/(Lev/OC_{bb})$ (10)

248 OC_{other} was calculated by balancing the ^{14}C content that was not attributed to
249 OC_{bb} .

250 $OC_{other} = (OC \times f_{nf}(OC) - OC_{bb} \times f_M(bb))/f_M(nf)$. (11)

251 Furthermore, $f_{nf}(OC)$ was calculated based on the ^{14}C concentration measured in
252 the sample (detailed description of the formulas can be found in Genberg et al., 2011);
253 $f_M(bb)$ and $f_M(nf)$ are the ^{14}C concentrations in biomass burning and other non-fossil
254 emissions, respectively.

255 Finally, OC_{ff} was calculated by subtraction (Eq. 9).

256 **2.9 Uncertainties of source apportionment**

257 Some uncertainties exist in some parameters in Eqs. 5–11 and need to be
258 evaluated. Table 1 lists the range of reference values used in this study. The ratios
259 Lev/OC_{bb} and EC_{bb}/OC_{bb} depend on the type of biofuel and the burning conditions
260 (Oros et al., 2001a, b). In foreign studies, the most common distributions of Lev/OC_{bb}



261 and EC_{bb}/OC_{bb} are 0.08–0.2 and 0.07–0.45, respectively (Gelencsér et al., 2007;
262 Puxbaum et al., 2007; Szidat et al., 2006). The distribution ranges of Lev/OC_{bb} and
263 EC_{bb}/OC_{bb} burned by trees, shrubs, and rice are approximately 0.01–0.04 and
264 0.05–0.31, respectively (Engling et al., 2006, 2009; Wang et al., 2009). Zhang et al.
265 (2007) found that the values of Lev/OC_{bb} and EC_{bb}/OC_{bb} in the cereal straw of BJ
266 were 0.08 and 0.13, respectively.

**Table 1. Values with limits of input parameters for source apportionment
using Latin hypercube sampling (LHS).**

Parameters	Low	Probable value	High
Lev/OC_{bb}	0.01	0.08	0.20
EC_{bb}/OC_{bb}	0.13	0.16	0.31
$\delta^{13}C_{liq.fossil}$ (‰)	−28.00	−27.00	−25.00
$\delta^{13}C_{Coal}$ (‰)	−25.00	−22.95	−21.00
$\delta^{13}C_{nf}^a$ (‰)	−26.00	−25.25	−24.00
$\delta^{13}C_{nf}^b$ (‰)	−27.00	−26.50	−25.00

Agnihotri et al., 2011; Engling et al., 2006, 2009; Gelencsér et al., 2007; Huang et al., 2006; Lopez-Veneroni, 2009; Martinelli et al., 2002; Moura et al., 2008; Oros et al., 2001a, b; Puxbaum et al., 2007; Smith & Epstein, 1971; Szidat et al., 2006; Turekian et al., 1998; Wang et al., 2009; Widory, 2006; Zhang et al., 2007.

^a Values used in BJ/LF

^b Values used in XA

267 The $\delta^{13}C$ of aerosols derived from liquid fossil fuels (gasoline and diesel oil) was
268 approximately −28 ‰ to −25 ‰ (Agnihotri et al., 2011; Huang et al., 2006;
269 Lopez-Veneroni, 2009; Widory, 2006). The $\delta^{13}C$ derived from coal combustion was
270 relatively high, ranging from −25 ‰ to −21 ‰ (Agnihotri et al., 2011; Widory, 2006).



271 The results of Agnihotri et al. (2011) showed that the $\delta^{13}\text{C}$ characteristic of biomass
272 burning emissions ranged from -25.9‰ to -29.4‰ . Smith & Epstein (1971) found
273 that plants with C3 (e.g., wheat, soybeans, and most woody plants) and C4 (e.g., corn,
274 grass, and sugar cane) metabolism had significantly different $\delta^{13}\text{C}$, with an average of
275 -27‰ and -13‰ , respectively. In other studies, these two types of plant-derived
276 aerosols had different characteristics; the ^{13}C from C3 and C4 plants ranged from
277 approximately -23.9‰ to -32‰ (Moura et al., 2008; Turekian et al., 1998) and
278 from -11.5‰ to -13.5‰ (Martinelli et al., 2002), respectively.

279 Because of the differences in the structure of biomass fuels in different cities, we
280 selected the $\delta^{13}\text{C}$ value based on the current status of biomass fuel used in research
281 regions. In China, biomass fuels mainly include crop residues, branches, and leaves,
282 and the amount of perennial wood is quite small (Zhang et al., 2015). BJ has a small
283 area of arable land, with low agricultural output and corn production (BJMBS, 2020).
284 The neighboring province, Hebei, is a large agricultural province that produces a large
285 amount of wheat and corn annually; the latter has a larger sown area (PGHP, 2020).
286 Shanxi Province also mainly produces wheat and corn; however, the sown area of
287 corn is more than three times that of wheat (SPBS, 2020). Agricultural production in
288 XA and the surrounding Guanzhong area is relatively large. The agricultural structure
289 is dominated by wheat and corn, and their sown areas are not very different (SAPBS,
290 2020). This shows that the $\delta^{13}\text{C}$ of agricultural straw burning in LF is likely to be
291 higher and that in XA may be lower. Some studies considered that $\delta^{13}\text{C}$ used for
292 quantitative mass–balance source apportionment calculations from biomass burning
293 should mainly be defined as C3 plants (Anderson et al., 2015; Fang et al., 2017; Ni et
294 al., 2020). Based on this information, the $\delta^{13}\text{C}$ value of biomass burning in BJ and LF
295 was found to be approximately -26‰ to -24‰ , and that in XA is likely to be from



296 approximately -27‰ to -25‰ .

297 Nuclear bomb tests in the late 1950s and the early 1960s released a large amount
298 of ^{14}C , and the ratio of $^{14}\text{C}/^{12}\text{C}$ in atmospheric CO_2 roughly doubled in the mid-1960s
299 (Hua & Barbetti, 2004; Levin et al., 2003, 2010; Lewis et al., 2004; Niu et al., 2021).
300 However, f_M in the atmosphere has been decreasing because of the dilution effect
301 produced by the absorption of marine and terrestrial biospheres and the release of
302 fossil fuels. In recent years, studies on background $^{14}\text{CO}_2$ in China and other countries
303 have shown that the f_M value in the atmosphere has decreased and approached 1
304 (Hammer et al., 2017; Niu et al., 2016). This means that the impact of the nuclear
305 explosions has almost disappeared, and the current changes in atmospheric ^{14}C are
306 mainly influenced by the regional natural carbon cycle and fossil fuel CO_2 emissions.
307 As perennial biomass fuel is less frequently used in China, the impact of nuclear
308 explosions on ^{14}C data can be ignored, and the $f_{M(\text{nf})}$ and $f_{M(\text{bb})}$ of the local station
309 should be close to the atmospheric value.

310 To evaluate the uncertainties of the quantification of source contributions, which
311 resulted from the uncertainties of the parameters used, we used Python software to
312 generate 3000 random variable simulations based on the LHS method (Gelencsér et
313 al., 2007). After excluding part of the out-of-range data, the median value of the
314 remaining simulations of each sample was considered as the best estimate. The results
315 of the uncertainties analysis is discussed further in Section 3.6.

316 **2.10 Air mass backward trajectory analysis**

317 For Backward trajectory analysis, air-mass back trajectories from the previous 48
318 h were determined by using the HYbrid Single-Particle Lagrangian Integrated
319 Trajectory (HYSPLIT) model (Draxler and Hess, 1998) at three different endpoint
320 heights (e.g., 100 m, 500 m, and 1000 m) and a time interval of 6 h for sampling day



321 (<https://www.arl.noaa.gov/>).

322

323 **3 Results and discussion**

324 **3.1 Characteristics and variation of carbonaceous components**

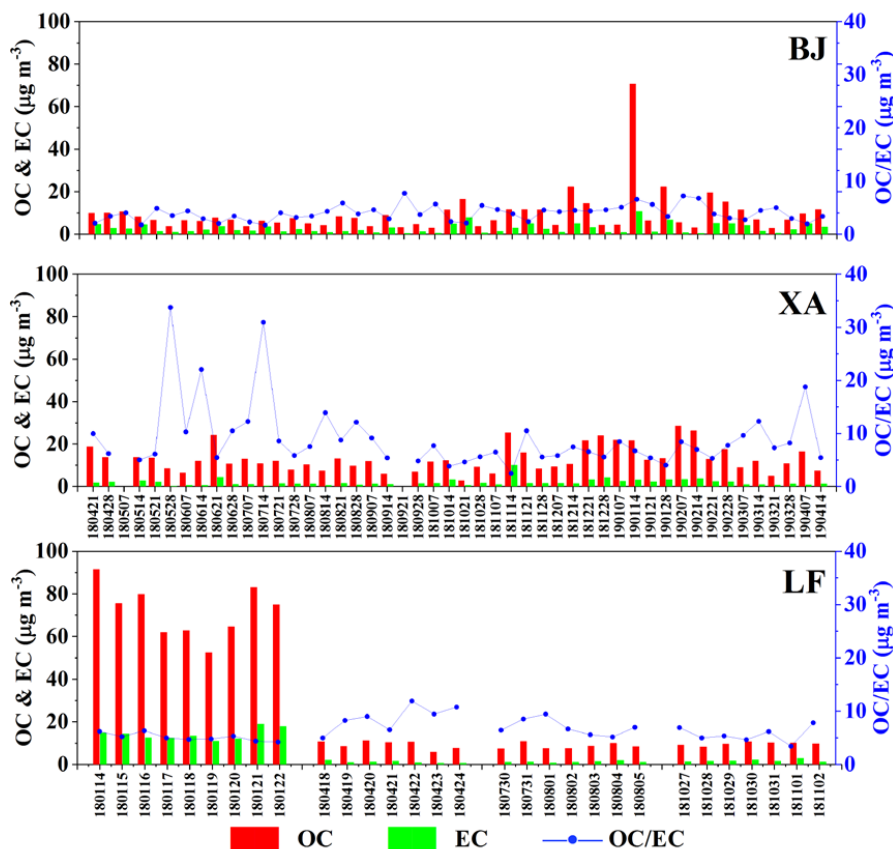
325 During the sampling period, the average mass concentration of PM_{2.5} in BJ, XA,
326 and LF was 72.07 ± 44.87 , 98.61 ± 64.53 , and 175.00 ± 134.41 $\mu\text{g m}^{-3}$, respectively.
327 All concentrations were higher in winter and lower in summer; LF showed the highest
328 value of 368.71 ± 74.96 $\mu\text{g m}^{-3}$ in winter.

329 Fig. 2 shows the changes in OC and EC and their ratios at the sampling sites. The
330 carbon components in the BJ, XA, and LF samples accounted for approximately 17.5
331 $\pm 6.0\%$, $21.5 \pm 21.0\%$, and $17.8 \pm 7.2\%$ of PM_{2.5}, respectively. Both OC and EC were
332 changing simultaneously and were characterized by low carbonaceous concentrations
333 in summer (OC: 8.85 ± 3.71 $\mu\text{g m}^{-3}$; EC: 1.56 ± 0.92 $\mu\text{g m}^{-3}$) and high concentrations
334 in winter (OC: 69.22 ± 58.94 $\mu\text{g m}^{-3}$; EC: 11.81 ± 7.88 $\mu\text{g m}^{-3}$). The average OC/EC
335 ratios in BJ, XA, and LF were 3.95 ± 1.41 , 8.98 ± 6.09 , and 6.58 ± 2.04 , respectively.
336 Recent studies have shown that the average ratio of OC/EC in BJ, XA, and Shanxi
337 Province was approximately 1.22–6.5 (Han et al., 2016; Ji et al., 2018; Wang et al.,
338 2015; Zhao et al., 2013). Generally, secondary OC (SOC) is considered to occur when
339 OC/EC > 2 (Castro et al., 1999; Novakov et al., 2005; Turpin & Huntzicker, 1995).
340 The high ratio indicates that all carbonaceous aerosols contained a large number of
341 SOCs, especially in XA.

342 The average mass concentrations of TC, OC, and EC at the sampling site in BJ
343 were 12.50 ± 11.79 , 9.73 ± 9.99 , and 2.77 ± 2.12 $\mu\text{gC m}^{-3}$. The concentration of
344 carbon components was relatively stable in spring and summer but fluctuated greatly
345 in autumn and winter. The concentration of carbon components in most cases was



346 close to that of other periods, but there was a rapid increase in autumn and winter. The
347 highest TC value was observed in the middle of January 2019 ($81.51 \mu\text{gC m}^{-3}$).



348

349 Fig. 2 Variations of carbon components and their ratios in $\text{PM}_{2.5}$ at the sampling sites
350 in Beijing (BJ), Xi'an (XA), and Linfen (LF) (date, "yymmdd").

351 The average concentrations of TC, OC, and EC in XA were 14.64 ± 7.52 , 12.76
352 ± 6.26 , and $1.89 \pm 1.61 \mu\text{gC m}^{-3}$, respectively. In contrast to that in BJ, the
353 concentration of the carbon components in XA fluctuated greatly throughout the year.
354 Specifically, the concentration was lower from July to October and significantly
355 higher from December to February. However, there were high concentrations of TC
356 on some days in spring and summer, such as June 21, 2018, with the concentration



357 reaching $28.75 \mu\text{gC m}^{-3}$.

358 The average concentrations of TC, OC, and EC in LF were 35.66 ± 36.53 , 30.03
359 ± 30.40 , and $5.64 \pm 6.24 \mu\text{gC m}^{-3}$, respectively. In contrast to those in BJ and XA, the
360 concentration of the carbon components in LF was persistently high in winter and
361 stable and low in other seasons.

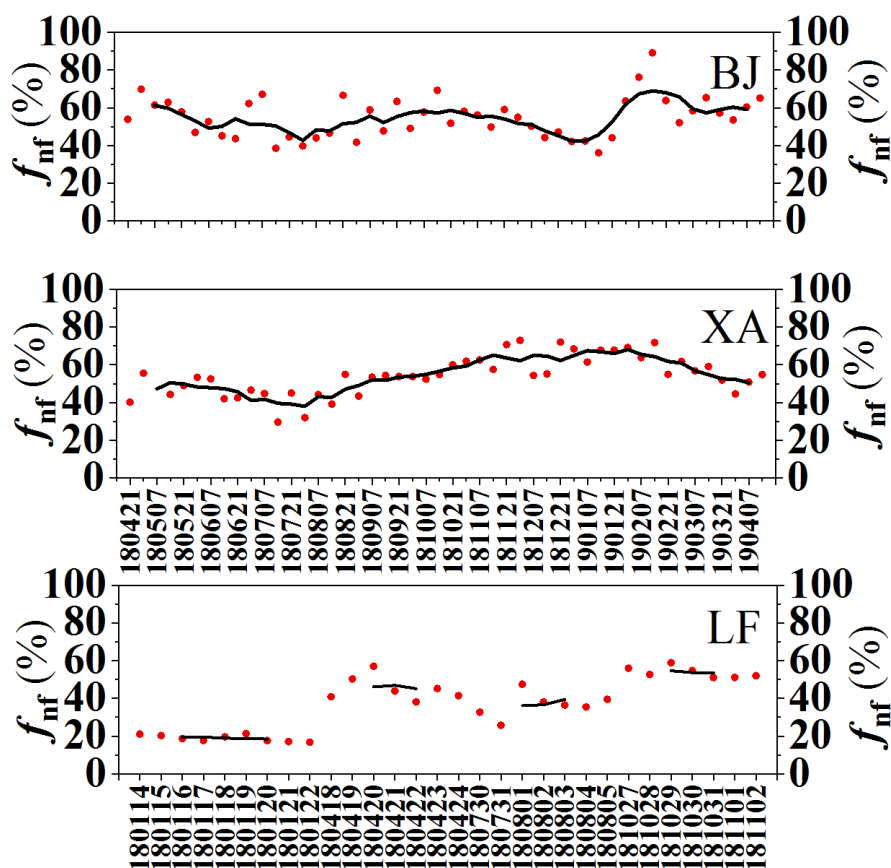
362 **3.2 Variations of ^{14}C**

363 The ^{14}C results showed that the average f_{nf} values in BJ, XA, and LF were $55 \pm$
364 11% , $54 \pm 10\%$, and $36 \pm 14\%$, respectively. Non-fossil sources were the main
365 contributors in the BJ and XA samples (Fig. 3). Furthermore, the f_{nf} in the BJ samples
366 showed a higher average value in spring ($59 \pm 6\%$), whereas that in the XA samples
367 had higher average values in autumn (f_{nf} , $59 \pm 7\%$) and winter (f_{nf} , $64 \pm 6\%$). In the
368 LF samples, fossil sources were the main contributors, contributing $80 \pm 1\%$ in
369 winter.

370 By analyzing the f_{nf} characteristics of samples with different pollution levels
371 based on the $\text{PM}_{2.5}$ concentration, we can study the causes and characteristics of air
372 pollution more effectively. Using the relevant classification index of the daily average
373 $\text{PM}_{2.5}$ concentration in the Technical Regulation on Ambient Air Quality Index (MEE,
374 2012), we divided the samples into clean (with a concentration of less than $75 \mu\text{g m}^{-3}$),
375 regular (with a concentration between 75 and $150 \mu\text{g m}^{-3}$), and polluted (with a
376 concentration greater than $150 \mu\text{g m}^{-3}$). The f_{nf} value in most samples in BJ ($44 \pm 8\%$)
377 and LF ($19 \pm 2\%$) was lower during serious air pollution (Fig. 4), indicating that the
378 high concentrations of aerosols in BJ and LF were more affected by fossil sources.
379 One BJ sample had a low f_{nf} value (36%) in January and another had a high f_{nf} value
380 (89%) in February. These samples were collected when the atmosphere was severely
381 polluted and very clean, respectively. This might indicate that emissions from fossil



382 fuel sources are a decisive factor of air pollution in BJ. In the XA samples, when the
383 atmosphere was clean, f_{nf} decreased by 2–3%, indicating that the carbonaceous
384 aerosol pollution may be more affected by biomass burning or secondary non-fossil
385 sources from local emissions.



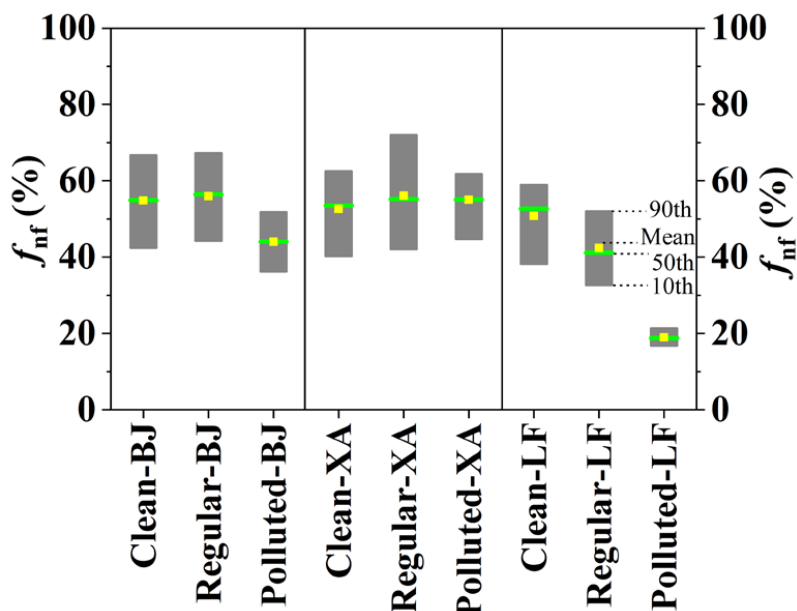
386
387 Fig. 3 Variations in proportion of non-fossil sources (f_{nf}) of carbonaceous aerosols at
388 the sampling sites in Beijing (BJ), Xi'an (XA), and Linfen (LF). The red scatter dot
389 represents the f_{nf} of each sample, and the black line represents the sliding average f_{nf}
390 value of every five samples (date, “yymmdd”).

391 Figure 5 lists the studies of ^{14}C in aerosols in our research area over the past few
392 decades. With the progress of air quality management, the proportion of fossil sources



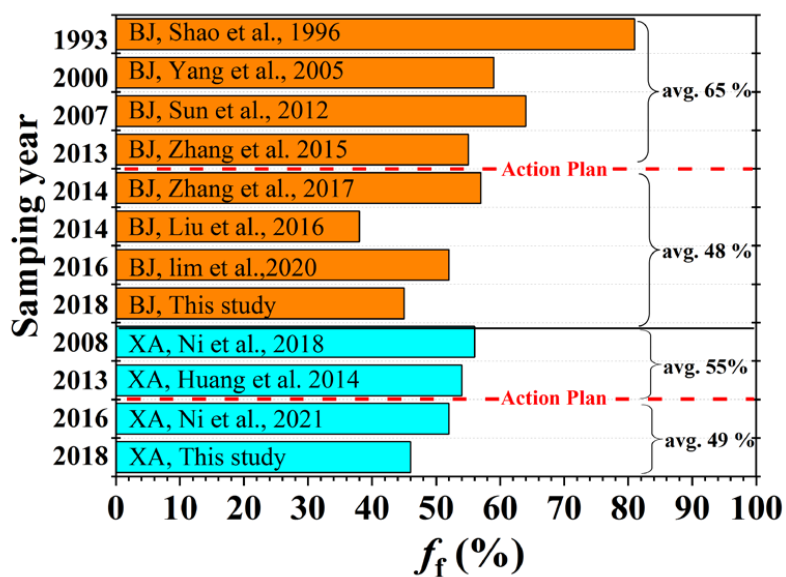
393 decreased by 6–17% in BJ and XA (Huang et al., 2014; Lim et al., 2020; Liu et al.,
394 2016; Ni et al., 2018, 2020; Shao et al., 1996; Sun et al., 2012; Yang et al., 2005;
395 Zhang et al., 2015, 2017). With the implementation of energy conservation and
396 emission reduction policies, many non-clean fossil fuels have been transformed into
397 clean energy. In 2019, the coal consumption in BJ was only 1.3 million tons, which
398 was 91.5% lower than that in 2013 (BJMBS, 2020). The decline in fossil source
399 contributions in XA (6%) was smaller than that in BJ (17%) in the past few decades.
400 This difference can be explained as follows: the decline in coal consumption in
401 Shaanxi Province during 2019 was not significant compared to that in 2013, whereas
402 the consumption of liquid fossil fuels decreased by 37% (SAPBS, 2020). The
403 particulate matter emitted from coal combustion is higher than that emitted from the
404 combustion of liquid fossil fuels (Chen et al., 2005; England et al., 2002; Guo et al.,
405 2014; Yan et al., 2010). Concerning non-fossil sources, China produces 939 million
406 tons of agricultural biomass residues annually, which is the main energy source for
407 some rural areas (Liao et al., 2004; Lu et al., 2009). In addition, the increase in urban
408 vegetation coverage may also increase the photochemical reactions of biological
409 volatile organic compounds (VOCs) (Gelencsér et al., 2007; NBS, 2021). Therefore,
410 in recent years, non-fossil fuels have gradually become a major contributor to
411 carbonaceous aerosols in BJ and XA with the reduction in the use of fossil energy.

412



413

414 Fig. 4 Boxplot distribution of f_{nf} of samples with different pollution levels. Clean
 415 samples: $PM_{2.5} < 75 \mu g m^{-3}$; regular samples: $75 \mu g m^{-3} \leq PM_{2.5} < 150 \mu g m^{-3}$;
 416 polluted samples: $PM_{2.5} \geq 150 \mu g m^{-3}$.



417



418 Fig. 5 Comparison of fossil proportion (f_f) of carbonaceous aerosol reported in
419 different studies in Beijing (BJ) and Xi'an (XA), China. The data has been converted
420 to the ratio of total carbon.

421

422 3.3 Air mass backward trajectory analysis

423 We analyzed and counted the backward trajectory during the sampling period;
424 several typical types are presented in Fig. S1. Figure S1 (a) shows the type of
425 backward trajectory with the highest frequency during the sample collection in BJ.
426 This type of long-distance transportation from the northwest accounted for
427 approximately 43.9% of all cases. The average $PM_{2.5}$ concentration, carbonaceous
428 aerosol concentration, and f_{nf} of the sample were $45.36 \pm 22.73 \mu\text{g m}^{-3}$, 9.52 ± 6.40
429 $\mu\text{gC m}^{-3}$, and $56 \pm 10\%$, respectively. As shown in Fig. S1 (b), when air mass was
430 transported from the south or stayed for a long time in the Hebei province, air
431 pollution was usually more serious. These cases accounted for approximately 26.3%
432 of all cases. The average concentrations of $PM_{2.5}$ and carbonaceous aerosols were
433 $97.30 \pm 43.61 \mu\text{g m}^{-3}$ and $15.60 \pm 7.94 \mu\text{gC m}^{-3}$, which were 2.1 and 1.6 times of
434 those in the northwest, respectively. The aerosol concentration of air masses
435 transported from the southern region was higher than that from the northern regions.
436 The f_{nf} value in these cases was $46 \pm 5\%$, which was 10% higher than in the northwest
437 cases. Thus, air pollution in BJ might be affected by fossil sources in the Hebei
438 province and other southern regions.

439 The $PM_{2.5}$ and carbonaceous concentrations were low when the air mass was
440 transported from the northwest for a long distance at the XA site (Fig. S1 (c)). In this
441 case, the average $PM_{2.5}$ concentration, carbonaceous aerosol concentration, and f_{nf} of
442 the samples were $93.05 \pm 65.1 \mu\text{g m}^{-3}$, $17.37 \pm 9.61 \mu\text{gC m}^{-3}$, and $62 \pm 7\%$,



443 respectively. However, when air masses circulated in the Guanzhong Basin owing to
444 topographical problems or converged into the basin from multiple directions (Fig. S1
445 (d)), the concentration of carbonaceous aerosol was usually high. The proportion of
446 this type of air mass transportation accounted for 53.6% of the total cases. The
447 average $PM_{2.5}$ concentration, carbonaceous aerosol concentration, and f_{nf} of the
448 corresponding samples were $131.95 \pm 72.75 \mu\text{g m}^{-3}$, $19.69 \pm 10.43 \mu\text{gC m}^{-3}$, and $58 \pm$
449 9% , respectively. Thus, air pollution in XA was mainly affected by the diffusion
450 environment. The air mass remained in the upper part of the Guanzhong region for a
451 long time when the diffusion environment was poor, causing secondary reactions and
452 air pollution. Moreover, when the air mass came from eastern cities (e.g., Henan or
453 Hubei provinces), f_{nf} was 47%, which was significantly lower than that in other cases.
454 This indicated that fossil source emissions in Henan and other eastern regions might
455 contribute to air pollution in XA.

456 As shown in Fig. S1 (e), when the air mass was long-distance transported to the
457 LF, the concentration of carbonaceous aerosols was relatively stable. However,
458 pollutants accumulated when the air mass returned over and around the city (Fig. S1
459 (f)). In these cases, the concentrations of $PM_{2.5}$ and carbonaceous aerosols of the
460 sample increased by 46.35–57.10%, and f_{nf} decreased by 5%. Thus, the LF samples
461 were more susceptible to the diffusion environment and the proportion of fossil
462 sources discharged locally.

463 Air pollution in BJ was more susceptible to the impact of transportation from the
464 southern region, whereas XA and LF were more affected by local emissions and
465 diffusion environments.

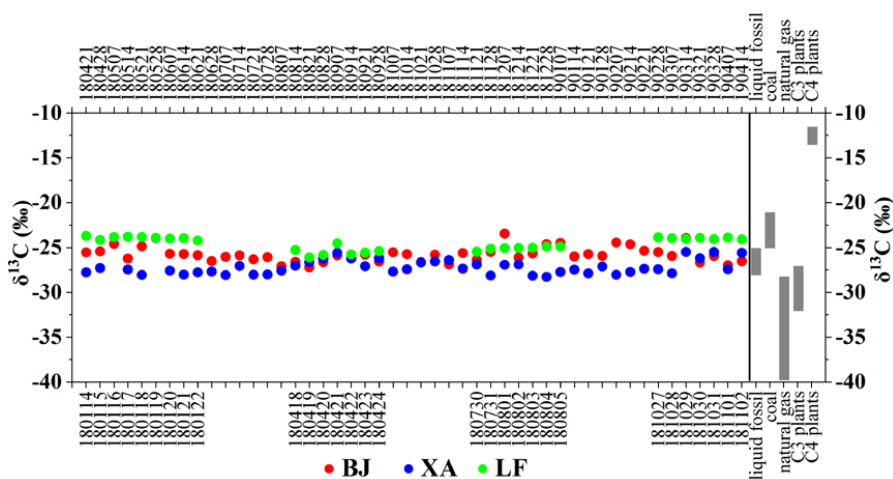
466

467 **3.4 Best estimate of source apportionment of TC using ^{14}C and ^{13}C**



468 The $\delta^{13}\text{C}$ values at the sampling sites in BJ, XA, and LF were $-25.83 \pm 0.81\text{‰}$,
 469 $-27.12 \pm 0.91\text{‰}$, and $-23.94 \pm 0.32\text{‰}$, respectively. Figure 6 shows the $\delta^{13}\text{C}$ values
 470 of the samples from each city and various sources. Specifically, $\delta^{13}\text{C}$ had lower values
 471 in the BJ and LF samples during summer ($-26.31 \pm 0.49\text{‰}$ and $-25.25 \pm 0.25\text{‰}$,
 472 respectively) and higher values during winter ($-25.17 \pm 0.79\text{‰}$ and $-23.94 \pm 0.16\text{‰}$,
 473 respectively). Conversely, the lower and higher $\delta^{13}\text{C}$ values in the XA samples
 474 appeared in winter ($-27.59 \pm 0.443\text{‰}$) and spring ($-26.54 \pm 1.23\text{‰}$).

475 Compared with the existing isotope indicators of various sources (Fig. 6), the
 476 increase in $\delta^{13}\text{C}$ in the BJ and LF samples during winter may be more related to the
 477 increase in coal combustion from local and the surrounding cities. The increase in
 478 $\delta^{13}\text{C}$ in XA samples during autumn and winter may be related to the use of C4 plant
 479 fuel, whereas the decrease during winter may be related to vehicle emissions and the
 480 use of C3 plant fuels, such as wheat straw or wood.



481 Fig. 6 $\delta^{13}\text{C}$ values of samples from Beijing (BJ), Xi'an (XA), and Linfen (LF), and
 482 comparison with the $\delta^{13}\text{C}$ distribution of various sources. The abscissa represents the
 483 sampling date (yyymmdd). The gray box indicates the $\delta^{13}\text{C}$ of the main source
 484



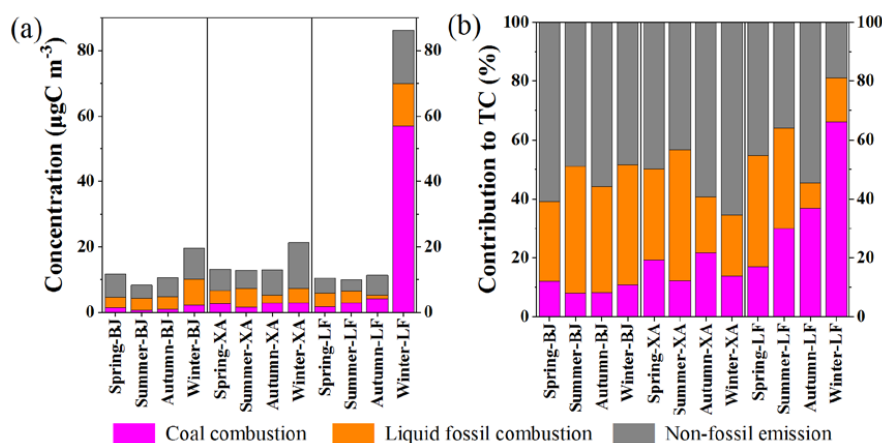
485 (Agnihotri et al., 2011; Huang et al., 2006; Lopez-Veneroni, 2009; Martinelli et al.,
486 2002; Moura et al., 2008; Smith & Epstein, 1971; Widory, 2006).

487 ^{14}C and ^{13}C were used to quantify the sources of TC in the carbonaceous aerosols
488 (Fig. 7). For the carbonaceous aerosols in BJ and XA, the best estimate of source
489 apportionment showed that the contributions of liquid fossil fuels were $33.6 \pm 12.9\%$
490 and $26.6 \pm 16.4\%$, respectively, which were greater than the contribution of coal (11.2
491 $\pm 9.1\%$ and $19.2 \pm 12.3\%$, respectively). In 2019, coal accounted for only 2.6% of all
492 fossil fuels used in BJ (BJMBS, 2020). This indicates that the local combustion of
493 coal was very low, and the coal contribution might be somewhat related to
494 transportation from the surrounding regions. Moreover, the higher contribution of
495 liquid fossil fuels in BJ was due to the high number of motor vehicles (6.4 million),
496 which was 1.7 times higher than that in XA in 2019 (BJMBS, 2020; XAMBS, 2020).
497 Figure S2 shows some studies on the source apportionment of coal and liquid fossil
498 fuels in aerosols in BJ over the past few decades. The coal contribution in BJ
499 decreased, whereas liquid fossil fuels gradually became the main source of fossil fuels.
500 After the implementation of the Action Plan, the proportion of coal in fossil sources
501 decreased by approximately 32% in BJ (Gao et al., 2018; Li et al., 2013; Liu et al.,
502 2014; Shang et al., 2019; Song et al., 2006; Tian et al., 2016; Wang et al., 2008;
503 Zhang et al., 2014).

504 In contrast, coal combustion contributed $39.2 \pm 20.5\%$ to LF samples, which was
505 greater than the contribution of liquid fossil emissions ($24.6 \pm 13.4\%$) and
506 significantly higher than those in BJ and XA. Especially in winter, coal contributed as
507 much as $66.2 \pm 3.6\%$ ($57.0 \pm 9.7 \mu\text{gC m}^{-3}$). According to the data released by the
508 Shanxi Provincial Bureau of Statistics, coal consumption in Shanxi Province was as
509 high as 349.06 million tons in 2019, which was 46.7 times of the consumption of



510 liquid fossil fuels, accounting for 70.3% of the total fossil fuel consumption (SPBS,
511 2020). The high contribution of coal combustion in winter might be related to the use
512 of household coal for heating by rural residents in Shanxi. This is because household
513 coal can emit a large amount of carbonaceous particles and is an important source of
514 carbonaceous aerosols in rural areas in northern China (Chen et al., 2005; Shen et al.,
515 2010; Streets et al., 2003; Zhi et al., 2008).



516
517 Fig. 7 Source apportionment of carbonaceous aerosols using radiocarbon (¹⁴C) and
518 stable carbon (¹³C) isotopes at the sampling sites in Beijing (BJ), Xi'an (XA), and
519 Linfen (LF) during different seasons. Red, blue, and orange represent the
520 concentrations and contributions of coal combustion, liquid fossil fuel, and non-fossil
521 sources emissions, respectively.

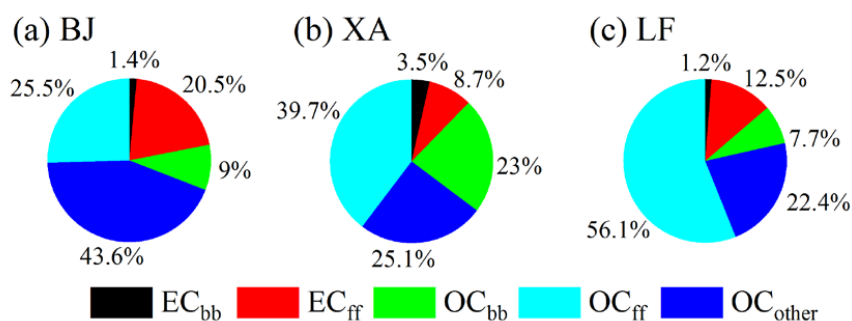
522

523 3.5 Best estimate of source apportionment of OC and EC by ¹⁴C and Lev

524 The concentration of each carbon component in BJ, XA, and LF was calculated
525 based on the combination of Lev and ¹⁴C. The best estimate of source apportionment
526 showed in Fig. 8. The contributions of OC_{other} (43.6 ± 12.9%), OC_{ff} (25.5 ± 11.7%),
527 and EC_{ff} (20.5 ± 6.5%) were relatively high in BJ. The OC_{bb} (23.0 ± 17.3%) and OC_{ff}



528 (39.7 ± 9.7%) were the highest contributors in XA. The LF samples showed different
529 characteristics, and the contribution of fossil sources was significantly high, especially
530 for the OC_{ff} (56.1 ± 11.9%).



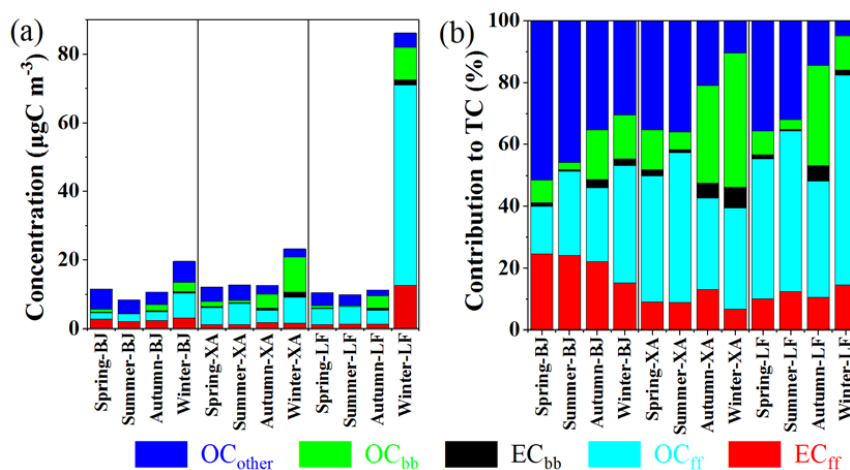
531 Fig. 8 Percentage of elemental carbon from biomass burning (EC_{bb}) and fossil-fuel
532 combustion (EC_{ff}) and percentage of organic carbon from biomass burning (OC_{bb}),
533 fossil-fuel combustion (OC_{ff}), and other sources (OC_{other}) for the PM_{2.5} samples in
534 Beijing (BJ), Xi'an (XA), and Linfen (LF).
535

536 3.5.1 Biomass burning contribution to TC

537 The concentrations ($0.22 \pm 0.27 \mu\text{gC m}^{-3}$) and contributions ($1.4 \pm 1.1\%$) of EC_{bb}
538 in BJ were relatively low during the whole year (Fig. 9). The EC_{bb} at the XA and LF
539 sites had high concentrations in autumn ($0.62 \pm 0.42 \mu\text{gC m}^{-3}$ and $0.58 \pm 0.09 \mu\text{gC m}^{-3}$)
540 and winter ($1.35 \pm 0.60 \mu\text{gC m}^{-3}$ and $1.53 \pm 0.21 \mu\text{gC m}^{-3}$) and low concentrations in
541 summer ($0.12 \pm 0.05 \mu\text{gC m}^{-3}$ and $0.05 \pm 0.02 \mu\text{gC m}^{-3}$), respectively. The OC_{bb}
542 concentrations in the BJ, XA, and LF samples showed an increase in autumn ($1.73 \pm$
543 $1.57 \mu\text{gC m}^{-3}$, $3.97 \pm 2.62 \mu\text{gC m}^{-3}$, and $3.63 \pm 0.55 \mu\text{gC m}^{-3}$) and winter (2.75 ± 2.33
544 $\mu\text{gC m}^{-3}$, $8.72 \pm 3.91 \mu\text{gC m}^{-3}$, and $9.57 \pm 1.33 \mu\text{gC m}^{-3}$), respectively. Especially in
545 the XA samples, OC_{bb} had high contributions in autumn ($32.4 \pm 13.9\%$) and winter
546 ($40.7 \pm 12.4\%$). The contribution of biomass combustion in XA ($26.5 \pm 19.9\%$) was
547 significantly larger than those in BJ ($10.4 \pm 8.3\%$) and LF ($9.0 \pm 11.0\%$), which was
548 also reflected in the concentration of Lev (Fig. S3). The Lev concentration in XA



549 $(0.35 \pm 0.40 \mu\text{g m}^{-3})$ was higher than that in BJ $(0.11 \pm 0.14 \mu\text{g m}^{-3})$ and slightly
550 higher than that in LF $(0.31 \pm 0.33 \mu\text{g m}^{-3})$. Furthermore, the Lev concentration in XA
551 during autumn and winter was up to 6.1 times higher than that during the other
552 seasons. Especially in winter, the proportion of Lev in the TC was $4.2 \pm 2.0\%$ in XA,
553 which was 3.7 and 4.5 times those in BJ and LF, respectively. Zhang et al. (2015)
554 attributed this to emissions from neighboring rural regions because such areas use
555 biofuels for heating and cooking more commonly in winter.



556
557 Fig. 9 Mass concentrations ($\mu\text{gC m}^{-3}$) (a) and percentage (b) of elemental carbon from
558 biomass burning (EC_{bb}) and fossil-fuel combustion (EC_{ff}) and organic carbon from
559 biomass burning (OC_{bb}), fossil-fuel combustion (OC_{ff}), and other sources (OC_{other}) for
560 carbonaceous aerosols samples in Beijing (BJ), Xi'an (XA), and Linfen (LF) during
561 different seasons.

562 3.5.2 Fossil contribution to TC

563 The EC_{ff} concentrations at BJ (spring: $2.76 \pm 1.41 \mu\text{gC m}^{-3}$; summer: 1.99 ± 0.84
564 $\mu\text{gC m}^{-3}$; autumn: $2.36 \pm 2.00 \mu\text{gC m}^{-3}$; winter: $3.00 \pm 2.72 \mu\text{gC m}^{-3}$) and XA (spring:
565 $1.14 \pm 0.73 \mu\text{gC m}^{-3}$; summer: $1.14 \pm 1.06 \mu\text{gC m}^{-3}$; autumn: $1.66 \pm 2.32 \mu\text{gC m}^{-3}$;
566 winter: $1.48 \pm 0.73 \mu\text{gC m}^{-3}$) did not fluctuate significantly during the year. The



567 concentration of EC_{ff} in LF during spring, summer, and autumn was relatively stable
568 ($1.05\text{--}1.24\ \mu\text{gC m}^{-3}$), but it was high during winter ($12.66 \pm 2.50\ \mu\text{gC m}^{-3}$), reaching
569 10.2 times that in summer.

570 The concentration of OC_{ff} was slightly higher in XA during summer (6.20 ± 2.20
571 $\mu\text{gC m}^{-3}$) and winter ($6.88 \pm 2.38\ \mu\text{gC m}^{-3}$). The contribution of OC_{ff} in the BJ
572 samples increased to $31.9 \pm 14.6\%$ during winter and decreased to $17.8 \pm 8.4\%$ during
573 spring. The OC_{ff}/EC_{ff} ratios in BJ and LF during winter were approximately 2.2 ± 1.2
574 and 4.7 ± 0.7 , respectively, suggesting that the fossil source secondary carbonaceous
575 aerosols were higher in winter. This could be explained by the lower temperature in
576 the winter altering the gas–particle equilibrium, suggesting that a larger portion of the
577 OC_{ff} during winter was secondary aerosol (Genberg et al., 2011). OC_{ff} in LF had high
578 concentrations in winter ($58.29 \pm 9.34\ \mu\text{gC m}^{-3}$) and low concentrations in summer
579 ($5.15 \pm 1.23\ \mu\text{gC m}^{-3}$). This indicated that the burning of fossil sources was an
580 important source of OC in BJ (OC_{ff} : $31.9 \pm 14.6\%$) and LF (OC_{ff} : $67.6 \pm 1.8\%$) during
581 winter. Fang et al. (2017) found that fossil fuels contributed significantly ($> 50\%$) to
582 carbon components in the haze in East Asia during January 2014, suggesting that the
583 aerosol contribution was generally dominated by fossil combustion sources. Therefore,
584 using cleaner energy and cleaner residential stoves to reduce and replace the
585 high-emission end-use coal combustion processes and control the emissions from
586 liquid-fossil-fueled vehicles in megacities should be beneficial to the air quality.

587 **3.5.3 Other non-fossil contributions to OC**

588 In addition to the OC directly emitted from fossil and biomass fuels, there are
589 many components of OC, such as SOC, whose source is difficult to identify.
590 Residential oil fume emissions from urban residents, emissions from biological
591 sources, and secondary bio-organic aerosols generated by the secondary reaction of



592 biomass fuels are also important components of OC (Gelencsér et al., 2007; Zhang et
593 al., 2015).

594 The concentration of OC_{other} in the LF samples did not vary greatly during spring
595 ($3.74 \pm 1.19 \mu\text{gC m}^{-3}$), summer ($3.17 \pm 0.53 \mu\text{gC m}^{-3}$), and winter ($4.06 \pm 2.55 \mu\text{gC}$
596 m^{-3}), but it was lower in autumn ($1.61 \pm 0.20 \mu\text{gC m}^{-3}$). In BJ, the contribution of
597 OC_{other} was high during spring ($51.0 \pm 9.3\%$), and its concentration was relatively
598 high during winter ($5.96 \pm 5.48 \mu\text{gC m}^{-3}$). Zhang et al. (2015) mainly attributed the
599 presence of OC_{other} in northern China to SOC formation from non-fossil, non-biogenic
600 precursors. In general, secondary bio-organic aerosols in spring and autumn are
601 mainly caused by biological emissions or long-distance transportation of biological
602 VOCs and secondary organic aerosols (SOAs) in particulates (Gelencsér et al., 2007;
603 Jimenez et al., 2009). The high concentration in winter may be because low
604 temperatures drive condensable semi-volatile organic compounds (SVOCs) into the
605 particulate phase (Simpson et al., 2007; Tanarit et al., 2008).

606 The OC_{other} contributions in XA were high in spring ($33.9 \pm 7.5\%$) and summer
607 ($34.9 \pm 10.1\%$). Some SOAs are formed by VOCs that are produced by burning wood
608 or biofuels (e.g., ethanol), and they increase the load of these sources on organic
609 aerosols (Genberg et al., 2011). Furthermore, SOC formation from these non-fossil
610 VOCs may be enhanced when they are mixed with other pollutants, such as VOCs
611 and NO_x (Hoyle et al., 2011; Weber et al., 2007). Motor vehicles are one of the main
612 anthropogenic sources of VOCs and NO_x (Barletta et al., 2005; Liu et al., 2008). We
613 found that motor vehicle emissions were higher in BJ and XA during winter and
614 summer, respectively (Fig. 7), which might explain the high concentration of OC_{other}
615 in BJ during winter and in XA during summer. Huang et al. (2014) found that severe
616 haze pollution was largely driven by secondary aerosol formation, and non-fossil

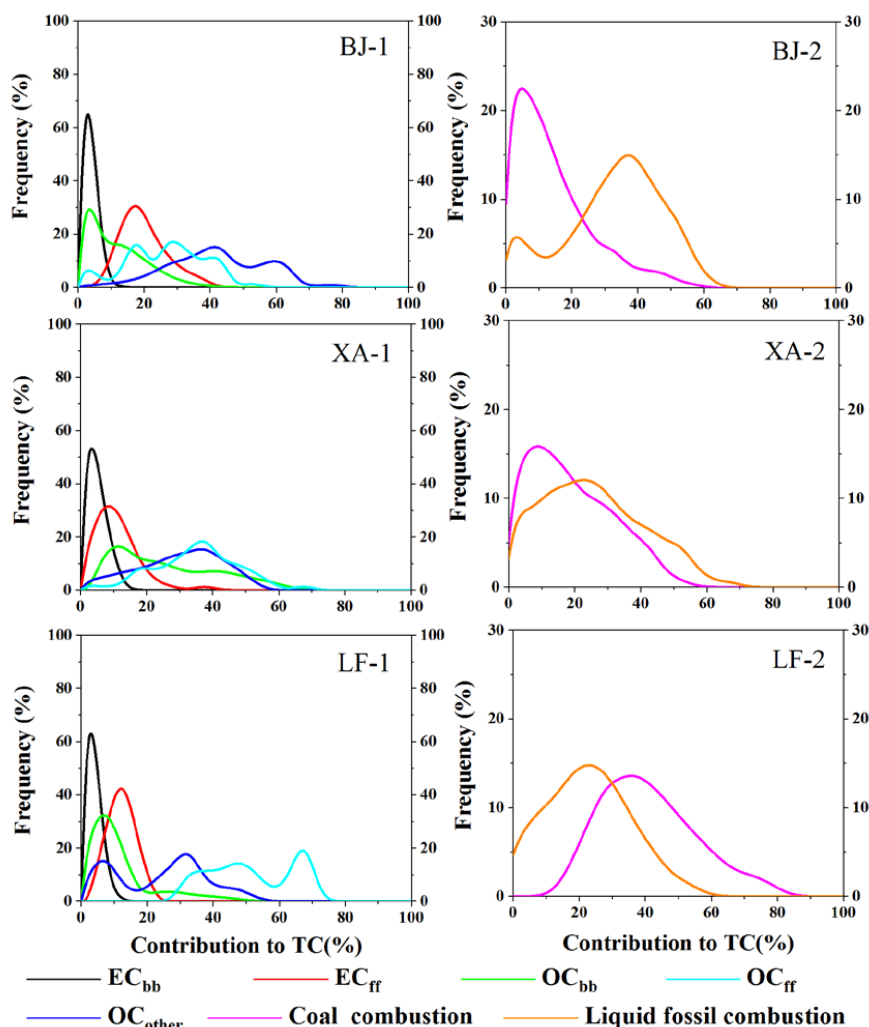


617 SOAs dominated, accounting for $66 \pm 8\%$ of the SOAs in XA despite extensive urban
618 emissions. Ni et al. (2020) also considered that non-fossil sources largely contributed
619 (56%) to SOC in XA. Thus, the control of biomass burning activities could be an
620 efficient strategy for reducing aerosols, especially in XA.

621

622 **3.6 Uncertainty analysis**

623 The results of the uncertainty analysis of the given set (Table 1) of the
624 parameters in the three cities are shown in Fig. 10. Each curve represents the
625 probability distribution of the sources of carbon components that contribute to the TC,
626 from which the uncertainty of the source allocation can be derived. Some results were
627 uncertain because the input parameters of the LHS calculation varied greatly. The
628 contributions of OC_{ff} and OC_{other} to the TC were mostly uncertain. This is mainly
629 related to the uncertainty of the two parameters, Lev/OC_{bb} and $(EC/OC)_{bb}$. Both these
630 parameters depend on the burning conditions and type of biomass, as mentioned in
631 Section 2.9. More reliable data would be obtained if $^{13}C/^{14}C$ could be performed on
632 the pure OC fractions of the samples, which has been proven to be feasible (Huang et
633 al., 2014; Szidat et al., 2004, 2006; Zhang et al., 2015). Other contributions have
634 single peaks, which proves that the results of the source analysis are reliable. These
635 results demonstrate that we can identify the main contributors.



636

637 Fig. 10 Latin hypercube sampling of frequency distributions of the source
638 contributions to total carbon (TC) from fossil, organic carbon (OC), and elemental
639 carbon (EC) source categories (Table 1) for the samples collected in Beijing (BJ),
640 Xi'an (XA), and Linfen (LF).

641

642 4 Conclusions

643 $PM_{2.5}$ samples were collected from BJ, XA, and LF in northern China from



644 January 2018 to April 2019. The main objective of this study was to quantify the
645 sources of carbonaceous aerosols by measuring the EC, OC, Lev, ^{13}C , and ^{14}C
646 combined with LHS.

647 The TC accounted for approximately $17.5 \pm 6\%$, $21.5 \pm 21\%$, and $17.8 \pm 7.2\%$ of
648 $\text{PM}_{2.5}$ in the samples from BJ, XA, and LF, and the corresponding concentrations
649 were $12.50 \pm 11.79 \mu\text{gC m}^{-3}$, $14.64 \pm 7.52 \mu\text{gC m}^{-3}$, and $35.66 \pm 36.53 \mu\text{gC m}^{-3}$,
650 respectively. The concentrations at the three sites showed high values in winter and
651 low values in summer. Based on backward trajectory analysis, we found that
652 carbonaceous aerosols in BJ were more susceptible to transportation from the
653 southern regions. Local emissions and the diffusion environment significantly
654 impacted carbonaceous aerosols in XA and LF.

655 The best estimate of source apportionment of the fossil components in the TC
656 showed that the contribution of liquid fossil fuel combustion was $33.6 \pm 12.9\%$ and
657 $26.6 \pm 16.4\%$ in BJ and XA, respectively, which was greater than the contribution of
658 coal combustion ($11.2 \pm 9.1\%$; $19.2 \pm 12.3\%$). In contrast, coal combustion
659 contributed $39.2 \pm 20.5\%$ in LF, which was greater than the contribution of liquid
660 fossil fuel combustion ($24.6 \pm 13.4\%$).

661 The best estimate of source apportionment of OC and EC indicated that the
662 contributions of EC_{ff} ($20.5 \pm 6.5\%$), OC_{ff} ($27.8 \pm 11.7\%$), and OC_{other} ($43.6 \pm 12.9\%$)
663 were relatively high in BJ. The OC_{ff} contribution was higher in winter ($31.9 \pm 14.6\%$),
664 and it was 3.4 times higher than that in other seasons. The contribution of OC_{bb} (23.0
665 $\pm 17.3\%$) and OC_{ff} ($39.7\% \pm 9.7\%$) was higher in XA. The contribution of biomass
666 burning to the TC was as high as $46.94 \pm 14.14\%$ in winter. The contribution of OC_{ff}
667 in LF was significantly high ($56.1 \pm 11.9\%$), especially in winter ($67.6 \pm 1.8\%$).

668 The decline (6–17%) in the contribution of fossil sources since the



669 implementation of the Action Plan indicates the effectiveness of air quality
670 management. In the future, the government needs to further regulate and control
671 emissions from motor vehicles in megacities such as BJ and XA. The cleaner use of
672 coal must be further strengthened in coal-based cities such as LF in the eastern part of
673 the Fenwei Plain. This study indicates that attention should be paid to the control of
674 biomass burning in northern China, especially in the Guanzhong region.

675

676 **Code and data availability:** The data products in this paper are available at the East
677 Asian Paleoenvironmental Science Database, National Earth System Science Data
678 Center, National Science & Technology Infrastructure of China
679 (http://paleodata.ieecas.cn/index_EN.aspx).

680

681 **Author contributions:** HZ performed the data analysis and wrote the initial draft of
682 the manuscript. ZN and WZ conceived the project and reviewed the paper. ZN and
683 SW provided the samples. HZ, XF, SW, XL and HD conducted the measurements. All
684 authors made substantial contributions to this work.

685

686 **Competing interests:** The authors declare that they have no conflict of interest.

687

688 **Acknowledgments:** The authors acknowledge the help of anonymous reviewers for
689 improving this article.

690

691 **Financial support:** The study was financially supported by the Strategic Priority
692 Research Program of the Chinese Academy of Sciences (XDA23010302), National
693 Research Program for Key Issues in Air Pollution Control (DQGG0105-02), the



694 National Natural Science Foundation of China (41773141, 42173082, and 41730108),
695 Natural Science Foundation of Shaanxi province (2014JQ2-4018), Key projects of
696 CAS (ZDRW-ZS-2017-6), and Natural Science Basic Research Program of Shaanxi
697 Province (2019JCW-20).

698

699 *References*

700 Agnihotri, R., Mandal, T., Karapurkar, S., Naja, M., Gadi, R., Ahammed, Y. N.,
701 Kumar, A., Saud, T., and Saxena, M.: Stable carbon and nitrogen isotopic
702 composition of bulk aerosols over India and northern Indian Ocean, *Atmospheric*
703 *Environment*, 45, 2828-2835, <https://doi.org/10.1016/j.atmosenv.2011.03.003>,
704 2011.

705 Andersson, A., Deng, J., Du, K., Zheng, M., Yan, C., Sköld, M., and Gustafsson, O. r.:
706 Regionally-varying combustion sources of the January 2013 severe haze events
707 over eastern China, *Environmental Science & Technology*, 49, 2038-2043,
708 <https://doi.org/10.1021/es503855e>, 2015.

709 Barletta, B., Meinardi, S., Rowland, F., Chan, C., Wang, X., Zou, S., Chan, L., and
710 Blake, D. R.: Volatile organic compounds in 43 Chinese cities, *Atmospheric*
711 *Environment*, 39, 5979-5990, <https://doi.org/10.1016/j.atmosenv.2005.06.029>,
712 2005.

713 BJMBS (Beijing Municipal Bureau Statistics): Beijing Statistical Yearbook-2020,
714 China Statistics
715 press., <http://nj.tjj.beijing.gov.cn/nj/main/2020-tjnj/zk/indexch.htm>, 2020 (last
716 access: 31 October 2021).

717 CaChier, H., Buat Menard, P., Fontugne, M., and Rancher, J.: Source terms and source
718 strengths of the carbonaceous aerosol in the tropics, *Journal of Atmospheric*



- 719 Chemistry, 3, 469-489, <https://doi.org/10.1007/BF00053872>, 1985.
- 720 Cachier, H., Buat Menard, P., Fontugne, M., and Chesselet, R.: Long-range transport
721 of continentally-derived particulate carbon in the marine atmosphere: Evidence
722 from stable carbon isotope studies, *Tellus B*, 38, 161-177,
723 <https://doi.org/10.1111/j.1600-0889.1986.tb00184.x>, 1986.
- 724 Cao, J., Lee, S., Ho, K., Zhang, X., Zou, S., Fung, K., Chow, J., and Watson, J.:
725 Characteristics of carbonaceous aerosol in Pearl River Delta Region, China
726 during 2001 winter period, *Atmospheric Environment*, 37, 1451-1460,
727 [https://doi.org/10.1016/S1352-2310\(02\)01002-6](https://doi.org/10.1016/S1352-2310(02)01002-6), 2003.
- 728 Cao, J., Lee, S., Chow, J., Watson, J., Ho, K., Zhang, R., Jin, Z., Shen, Z., Chen, G.,
729 and Kang, Y.: Spatial and seasonal distributions of carbonaceous aerosols over
730 China, *Journal of Geophysical Research Atmospheres*, D112, 22-11,
731 <https://doi.org/10.1029/2006JD008205>, 2007.
- 732 Cao, J., Zhu, C., Chow, J., Watson, J., Han, Y., Wang, G., Shen, Z., and An, Z.: Black
733 carbon relationships with emissions and meteorology in Xi'an, China,
734 *Atmospheric Research*, 94, 194-202, <https://doi.org/10.1029/2006JD008205>,
735 2009.
- 736 Cao, J., Chow, J., Tao, J., Lee, S., Watson, J., Ho, K., Wang, G., Zhu, C., and Han, Y.:
737 Stable carbon isotopes in aerosols from Chinese cities: Influence of fossil fuels,
738 *Atmospheric Environment*, <https://doi.org/10.1016/j.atmosenv.2010.10.056>,
739 2011.
- 740 Castro, L., Pio, C., Harrison, R., and Smith, D.: Carbonaceous aerosol in urban and
741 rural European atmospheres: estimation of secondary organic carbon
742 concentrations, *Atmospheric Environment*, 33, 2771-2781,
743 <https://doi.org/10.5194/acpd-11-2749-2011>, 1999.



- 744 CCTV (China Central Television): The concentration of SO₂ in Linfen, Shanxi
745 exceeded 1,000 again, and no early warning measures have been
746 issued., [http://news.cctv.com/2017/01/10/ARTI4FWBKnxduEq7kDOGIceD1701](http://news.cctv.com/2017/01/10/ARTI4FWBKnxduEq7kDOGIceD170110.shtml)
747 [10.shtml](http://news.cctv.com/2017/01/10/ARTI4FWBKnxduEq7kDOGIceD170110.shtml), 2017 (last access: 31 October 2021).
- 748 Ceburnis, D., Garbaras, A., Szidat, S., Rinaldi, M., Fahrni, S., Perron, N., Wacker, L.,
749 Leinert, S., Remeikis, V., and Facchini, M. C.: Quantification of the
750 carbonaceous matter origin in submicron marine aerosol particles by dual carbon
751 isotope analysis, 11, 8593-8606, <https://doi.org/10.5194/acpd-11-2749-2011>,
752 2011.
- 753 Chen, Y., Sheng, G., Bi, X., Feng, Y., Mai, B., and Fu, J.: Emission Factors for
754 Carbonaceous Particles and Polycyclic Aromatic Hydrocarbons from Residential
755 Coal Combustion in China, *Environmental Science & Technology*, 39,
756 1861-1867, <https://doi.org/10.1021/es0493650>, 2005.
- 757 Chesselet, R., Fontugne, M., Menard, P. B., Ezat, U., and Lambert, C. E.: The origin
758 of particulate organic carbon in the marine atmosphere as indicated by its stable
759 carbon isotopic composition, *Geophysical Research Letters*, 8,
760 <https://doi.org/10.1029/GL008i004p00345>, 2013.
- 761 Chow, J., and Watson, J.: PM_{2.5} carbonate concentrations at regionally representative
762 Interagency Monitoring of Protected Visual Environment sites, *Journal of*
763 *Geophysical Research Atmospheres*, 107, <https://doi.org/10.1029/2001JD000574>,
764 2002.
- 765 Chow, J., Watson, J., Chen, L., Arnott, W., Moosmüller, H., and Fung, K.:
766 Equivalence of Elemental Carbon by Thermal/Optical Reflectance and
767 Transmittance with Different Temperature Protocols, *Environmental Science &*
768 *Technology*, 38, 4414-4422, <https://doi.org/10.1021/es034936u>, 2004.



- 769 Claeys, M., Kourtchev, I., Pashynska, V., Vas, G., Vermeulen, R., Wang, W., Cafmeyer,
770 J., Chi, X., Artaxo, P., and Andreae, M. O.: Polar organic marker compounds in
771 atmospheric aerosols during the LBA-SMOCC 2002 biomass burning
772 experiment in Rondônia, Brazil: sources and source processes, time series, diel
773 variations and size distributions, *Atmospheric Chemistry & Physics*,
774 <https://doi.org/10.5194/acp-10-9319-2010>, 2010.
- 775 Clarke, A., and Karani, G.: Characterisation of the carbonate content of atmospheric
776 aerosols, *Journal of Atmospheric Chemistry*, 14, 119-128,
777 <https://doi.org/10.1007/BF00115228>, 1992.
- 778 Clayton, G., Arnold, J., and Patty, F.: Determination of Sources of Particulate
779 Atmospheric Carbon, *Science*, 122, 751-753,
780 <https://doi.org/10.1126/science.122.3173.751>, 1955.
- 781 Coplen, T.: New guidelines for reporting stable hydrogen, carbon, and oxygen
782 isotope-ratio data, *Geochimica et Cosmochimica Acta*, 60, 3359-3360,
783 [https://doi.org/10.1016/0016-7037\(96\)00263-3](https://doi.org/10.1016/0016-7037(96)00263-3), 1996.
- 784 CSC (Chinese State Council): Action Plan for Air Pollution Prevention and
785 Control. , http://www.gov.cn/zhengce/content/2013-09/13/content_4561.htm,
786 2013 (last access: 31 October 2021).
- 787 CSC (Chinese State Council): Three-year action plan to fight air pollution (NO. 2018.
788 22). , http://www.gov.cn/zhengce/content/2018-07/03/content_5303158.htm .
789 2018 (last access: 31 October 2021).
- 790 Currie, L.: Evolution and Multidisciplinary Frontiers of ¹⁴C Aerosol Science 1,
791 *Radiocarbon*, 42, 115-126, 2000.
- 792 Draxler, R., and Hess, G.: An overview of the HYSPLIT_4 modelling system for
793 trajectories, *Australian meteorological magazine*, 47, 295-308, 1998.



- 794 England, G.: Development of fine particulate emission factors and speciation profiles
795 for oil and gas-fired combustion systems, GE Energy and Environmental
796 Research Corporation (US), 2004.
- 797 Engling, G., Carrico, C., Kreidenweis, S., Collett Jr., J., Day, D., C. Malm, W., Lincoln,
798 E., Hao, W., Iinuma, Y., and Herrmann, H.: Determination of levoglucosan in
799 biomass combustion aerosol by high-performance anion-exchange
800 chromatography with pulsed amperometric detection, *Atmospheric Environment*,
801 2006, 40, S299-S311, <https://doi.org/10.1016/j.atmosenv.2005.12.069>, 2006.
- 802 Engling, G., Lee, J. J., Tsai, Y., Lung, S., C., C., Chou, C., and Chan, C.:
803 Size-Resolved Anhydrosugar Composition in Smoke Aerosol from Controlled
804 Field Burning of Rice Straw, *Aerosol Science & Technology*, 43, 662-672,
805 <https://doi.org/10.1080/02786820902825113>, 2009.
- 806 Fang, W., Andersson, A., Zheng, M., Lee, M., Holmstrand, H., Kim, S., Du, K., and
807 Örjan, G.: Divergent Evolution of Carbonaceous Aerosols during Dispersal of
808 East Asian Haze, *Scientific Reports*, 7, 10422,
809 <https://doi.org/10.1038/s41598-017-10766-4>, 2017.
- 810 Feng, Y., Chen, Y., Hui, G., Zhi, G., Xiong, S., Li, J., Sheng, G., and Fu, J.:
811 Characteristics of organic and elemental carbon in PM_{2.5} samples in Shanghai,
812 China, *Atmospheric Research*, 92, 434-442,
813 <https://doi.org/10.1016/j.atmosres.2009.01.003>, 2009.
- 814 Gao, J., Wang, K., Wang, Y., Liu, S., Zhu, C., Hao, J., Liu, H., Hua, S., and Tian, H.:
815 Temporal-spatial characteristics and source apportionment of PM_{2.5} as well as
816 its associated chemical species in the Beijing-Tianjin-Hebei region of China,
817 *Environmental pollution*, 233, 714-724,
818 <https://doi.org/10.1016/j.envpol.2017.10.123>, 2018.



- 819 Gelencsér, A., May, B., Simpson, D., Sánchez-Ochoa, A., Kasper-Giebl, A., Puxbaum,
820 H., Caseiro, A., Pio, C., and Legrand, M.: Source apportionment of PM_{2.5}
821 organic aerosol over Europe: Primary/secondary, natural/anthropogenic, and
822 fossil/biogenic origin, *Journal of Geophysical Research: Atmospheres*, 112,
823 <https://doi.org/10.1029/2006jd008094>, 2007.
- 824 Genberg, J., Hyder, M., Stenström, K., Bergström, R., Simpson, D., Fors, E., Jönsson,
825 J., and Swietlicki, E.: Source apportionment of carbonaceous aerosol in southern
826 Sweden, *Atmospheric Chemistry & Physics*, 11, 13575-13616,
827 <https://doi.org/10.5194/acp-11-11387-2011>, 2011.
- 828 Guo, J., Ge, Y., Hao, L., Tan, J., Li, J., and Feng, X.: On-road measurement of
829 regulated pollutants from diesel and CNG buses with urea selective catalytic
830 reduction systems, *Atmospheric Environment*,
831 <https://doi.org/10.1016/j.atmosenv.2014.07.032>, 2014.
- 832 Hammer, S., and Levin, I.: Monthly mean atmospheric D₁₄CO₂ at Jungfrauoch and
833 Schauinsland from 1986 to 2016, *Tellus B*, 65, 20092,
834 <https://doi.org/10.11588/data/10100>, 2017.
- 835 Han, Y., Chen, L., Huang, R., Chow, J., Watson, J., Ni, H., Liu, S., Fung, K., Shen, Z.,
836 and Wei, C.: Carbonaceous aerosols in megacity Xi'an, China: Implications of
837 thermal/optical protocols comparison, *Atmospheric Environment*,
838 <https://doi.org/10.1016/j.atmosenv.2016.02.023>, 2016.
- 839 Hoffmann, D., Tilgner, A., Iinuma, Y., and Herrmann, H.: Atmospheric stability of
840 levoglucosan: a detailed laboratory and modeling study, *Environmental Science
& Technology*, 44, 694-699, <https://doi.org/10.1021/es902476f>, 2010.
- 842 Hoyle, C., Boy, M., Donahue, N., Fry, J., Glasius, M., Guenther, A., Hallar, A., Hartz,
843 K. H., Petters, M., Petäjä, T., Rosenoern, T., and Sullivan, A.: A review of the



- 844 anthropogenic influence on biogenic secondary organic aerosol, *Atmospheric*
845 *Chemistry & Physics*, 11, <https://doi.org/10.5194/acp-11-321-2011>, 2011.
- 846 Hua, Q., and Barbetti, M.: Review of Tropospheric Bomb ¹⁴C Data for Carbon Cycle
847 Modeling and Age Calibration Purposes, *Radiocarbon*, 46,
848 <https://doi.org/10.1017/S0033822200033142>, 2004.
- 849 Huang, J., Kang, S., Shen, C., Cong, Z., Liu, K., Wang, W., and Liu, L.: Seasonal
850 variations and sources of ambient fossil and biogenic-derived carbonaceous
851 aerosols based on ¹⁴C measurements in Lhasa, Tibet, *Atmospheric Research*, 96,
852 553-559, <https://doi.org/10.1016/j.atmosres.2010.01.003>, 2010.
- 853 Huang, L., Brook, J., Zhang, W., Li, S., Graham, L., Ernst, D., Chivulescu, A., and Lu,
854 G.: Stable isotope measurements of carbon fractions (OC/EC) in airborne
855 particulate: A new dimension for source characterization and apportionment,
856 *Atmospheric Environment*, 40, 2690-2705,
857 <https://doi.org/10.1016/j.atmosenv.2005.11.062>, 2006.
- 858 Huang, R., Zhang, Y., Bozzetti, C., Ho, K., Cao, J., Han, Y., Dällenbach, K. R.,
859 Slowik, J. G., Platt, S. M., Canonaco, F., Zotter, P., Wolf, R., Pieber, S. M., Bruns,
860 E. A., Crippa, M., Ciarelli, G., Piazzalunga, A., Schwikowski, M., Abbaszade, G.,
861 Schnelle-Kreis, J., Zimmermann, R., An, Z., Szidat, S., Baltensperger, U.,
862 Haddad, I. E., and Prévôt, A.: High secondary aerosol contribution to particulate
863 pollution during haze events in China, *Nature*, 514, 218-222,
864 <https://doi.org/10.1038/nature13774>, 2014.
- 865 Jacobson, M.: Strong radiative heating due to the mixing state of black carbon in
866 atmospheric aerosols, *Nature*, 2001.
- 867 Jacobson, M. C., Hansson, H. C., Noone, K. J., and Charlson, R. J.: Organic
868 atmospheric aerosols: Review and state of the science, *Reviews of Geophysics*,



- 869 38, 267-294, <https://doi.org/10.1029/1998RG000045>, 2000.
- 870 Ji, D., Yan, Y., Wang, Z., He, J., Liu, B., Sun, Y., Gao, M., Li, Y., Cao, W., and Cui, Y.:
- 871 Two-year continuous measurements of carbonaceous aerosols in urban Beijing,
- 872 China: Temporal variations, characteristics and source analyses, *Chemosphere*,
- 873 200, 191-200, <https://doi.org/10.1016/j.chemosphere.2018.02.067>, 2018.
- 874 Jimenez, J., Canagaratna, M., Donahue, N., Prevot, A., Zhang, Q., Kroll, J., DeCarlo,
- 875 P., Allan, J., Coe, H., Ng, N., Aiken, A., Docherty, K., Ulbrich, I., Grieshop, A.,
- 876 Robinson, A., Duplissy, J., Smith, J., Wilson, K., Lanz, V., Hueglin, C., Sun, Y.,
- 877 Tian, J., Laaksonen, A., Raatikainen, T., Rautiainen, J., Vaattovaara, P., Ehn, M.,
- 878 Kulmala, M., Tomlinson, J., Collins, D., Cubison, M., Dunlea, J., Huffman, J.,
- 879 Onasch, T., Alfarra, M., Williams, P., Bower, K., Kondo, Y., Schneider, J.,
- 880 Drewnick, F., Borrmann, S., Weimer, S., Demerjian, K., Salcedo, D., Cottrell, L.,
- 881 Griffin, R., Takami, A., Miyoshi, T., Hatakeyama, S., Shimono, A., Sun, J.,
- 882 Zhang, Y., Dzepina, K., Kimmel, J., Sueper, D., Jayne, J., Herndon, S., Trimborn,
- 883 A., Williams, L., Wood, E., Middlebrook, A., Kolb, C., Baltensperger, U., and
- 884 Worsnop, D.: Evolution of Organic Aerosols in the Atmosphere, *Science*, 326,
- 885 1525-1529, doi:10.1126/science.1180353, 2009.
- 886 Jull, A.: Radiocarbon dating| AMS method, in: *Encyclopedia of Quaternary science*,
- 887 Elsevier Science Ltd., 2911-2918, 2006.
- 888 Kawashima, H., and Haneishi, Y.: Effects of combustion emissions from the Eurasian
- 889 continent in winter on seasonal $\delta^{13}\text{C}$ of elemental carbon in aerosols in Japan,
- 890 *Atmospheric Environment*, 46, 568-579,
- 891 <https://doi.org/10.1016/j.atmosenv.2011.05.015>, 2012.
- 892 Kiehl, and Jeffrey, T.: Twentieth century climate model response and climate
- 893 sensitivity, *Geophysical Research Letters*, 34, 22710, 2007.



- 894 Kirillova, E., Andersson, A., Sheesley, R., Kruså, M., Praveen, P., Budhavant, K.,
895 Safai, P., Rao, P., and Gustafsson, Ö.: 13C- And 14C-based study of sources and
896 atmospheric processing of water-soluble organic carbon (WSOC) in South Asian
897 aerosols, *Journal of Geophysical Research Atmospheres*, 118, 614-626,
898 <https://doi.org/10.1002/jgrd.50130>, 2013.
- 899 Kumagai, K., Iijima, A., Shimoda, M., Saitoh, Y., Kozawa, K., Hagino, H., and
900 Sakamoto, K.: Determination of Dicarboxylic Acids and Levoglucosan in Fine
901 Particles in the Kanto Plain, Japan, for Source Apportionment of Organic
902 Aerosols, *Aerosol & Air Quality Research*, 10, 282-291,
903 <https://doi.org/10.4209/aaqr.2009.11.0075>, 2010.
- 904 Levin, I., Kromer, B., Schmidt, M., and Sartorius, H.: A novel approach for
905 independent budgeting of fossil fuel CO₂ over Europe by 14CO₂ observations,
906 *Geophysical Research Letters*, 30, <https://doi.org/10.1029/2003GL018477>, 2003.
- 907 Levin, I., Naegler, T., Kromer, B., Diehl, M., Francey, R., Gomez Pelaez, A., Steele, P.,
908 Wagenbach, D., Weller, R., and Worthy, D.: Observations and modelling of the
909 global distribution and long-term trend of atmospheric 14CO₂, *Tellus B*, 62,
910 26-46, <https://doi.org/10.1111/j.1600-0889.2009.00446.x>, 2010.
- 911 Lewis, C., Klouda, G., and Ellenson, W.: Radiocarbon measurement of the biogenic
912 contribution to summertime PM-2.5 ambient aerosol in Nashville, TN,
913 *Atmospheric Environment*, 38, 6053-6061,
914 <https://doi.org/10.1016/j.atmosenv.2004.06.011>, 2004.
- 915 Li, C., Bosch, C., Kang, S., Andersson, A., Chen, P., Zhang, Q., Cong, Z., Chen, B.,
916 Qin, D., and Gustafsson, Ö.: Sources of black carbon to the Himalayan-Tibetan
917 Plateau glaciers, *Nature Communications*, 7, 12574,
918 <https://doi.org/10.1038/ncomms12574>, 2016.



- 919 Li, X., Wang, Y., Guo, X., and Wang, Y.: Seasonal variation and source apportionment
920 of organic and inorganic compounds in PM_{2.5} and PM₁₀ particulates in Beijing,
921 China, *Journal of Environmental Sciences*, 25, 741-750,
922 [https://doi.org/10.1016/S1001-0742\(12\)60121-1](https://doi.org/10.1016/S1001-0742(12)60121-1), 2013.
- 923 Liao, C., Wu, C., Yanyongjie, and Huang, H.: Chemical elemental characteristics of
924 biomass fuels in China, *Biomass and Bioenergy*, 27, 119-130,
925 <https://doi.org/10.1016/j.biombioe.2004.01.002>, 2004.
- 926 Lim, S., Yang, X., Lee, M., Li, G., and Jeon, K.: Fossil-driven secondary inorganic
927 PM_{2.5} enhancement in the North China Plain: Evidence from carbon and
928 nitrogen isotopes, *Environmental Pollution*, 266, 115163,
929 <https://doi.org/10.1016/j.envpol.2020.115163>, 2020.
- 930 Liu, D., Li, J., Zhang, Y., Xu, Y., Liu, X., Ping, D., Shen, C., Chen, Y., Tian, C., and
931 Zhang, G.: The Use of Levoglucosan and Radiocarbon for Source
932 Apportionment of PM_{2.5} Carbonaceous Aerosols at a Background Site in East
933 China, *Environmental Science & Technology*, 47,
934 <https://doi.org/10.1021/es401250k>, 2013.
- 935 Liu, J., Li, J., Zhang, Y., Liu, D., Ding, P., Shen, C., Shen, K., He, Q., Ding, X., Wang,
936 X., Chen, D., Szidat, S. n., and Zhang, G.: Source Apportionment Using
937 Radiocarbon and Organic Tracers for PM_{2.5} Carbonaceous Aerosols in
938 Guangzhou, South China: Contrasting Local- and Regional-Scale Haze Events,
939 *Environmental Science & Technology*, 48, 12002-12011,
940 <https://doi.org/10.1021/es503102w>, 2014.
- 941 Liu, J., Mo, Y., Li, J., Liu, D., Shen, C., Ding, P., Jiang, H., Cheng, Z., Zhang, X., and
942 Tian, C.: Radiocarbon-derived source apportionment of fine carbonaceous
943 aerosols before, during, and after the 2014 Asia-Pacific Economic Cooperation



944 (APEC) summit in Beijing, China, *Journal of Geophysical Research:*
945 *Atmospheres*, 121, 4177-4187, <https://doi.org/10.5194/acp-16-2985-2016>, 2016.

946 Liu, Y., Shao, M., Fu, L., Lu, S., Zeng, L., and Tang, D.: Source profiles of volatile
947 organic compounds (VOCs) measured in China: Part I, *Atmospheric*
948 *Environment*, 42, 6247-6260, <https://doi.org/10.1016/j.atmosenv.2008.01.070>,
949 2008.

950 Liu, Z., Hu, B., Liu, Q., Sun, Y., and Wang, Y.: Source apportionment of urban fine
951 particle number concentration during summertime in Beijing, *Atmospheric*
952 *Environment*, 96, 359-369, <https://doi.org/10.1016/j.atmosenv.2014.06.055>,
953 2014.

954 Locker, H. B.: The use of levoglucosan to assess the environmental impact of
955 residential wood-burning on air quality, Hanover, NH (US); Dartmouth College,
956 1988.

957 Lopez-Veneroni, D.: The stable carbon isotope composition of PM_{2.5} and PM₁₀ in
958 Mexico City Metropolitan Area air, *Atmospheric Environment*, 43, 4491-4502,
959 <https://doi.org/10.1016/j.atmosenv.2009.06.036>, 2009.

960 Lu, L., Tang, Y., Xie, J., and Yuan, Y.: The role of marginal agricultural land-based
961 mulberry planting in biomass energy production, *Renewable Energy*, 34,
962 1789-1794, <https://doi.org/10.1016/j.renene.2008.12.017>, 2009.

963 Martinelli, L., Camargo, P., Lara, L., Victoria, R., and Artaxo, P.: Stable carbon and
964 nitrogen isotopic composition of bulk aerosol particles in a C₄ plant landscape of
965 southeast Brazil, *Atmospheric Environment*, 36, 2427-2432,
966 [https://doi.org/10.1016/S1352-2310\(01\)00454-X](https://doi.org/10.1016/S1352-2310(01)00454-X), 2002.

967 MEE (Ministry of Ecology and Environment of the People's Republic of China):
968 Technical Regulation on Ambient Air Quality Index, China Environmental



969 Science Press (HJ 633–2012), 2012 (last access: 31 October 2021).

970 MEE (Ministry of Ecology and Environment of the People's Republic of China):
971 Bulletin of Ecology and Environment of the People's Republic of China 2013. ,
972 2014 (last access: 31 October 2021).

973 MEE (Ministry of Ecology and Environment of the People's Republic of China):
974 Bulletin of Ecology and Environment of the People's Republic of China 2018. ,
975 2019 (last access: 31 October 2021).

976 MEE (Ministry of Ecology and Environment of the People's Republic of China):
977 Bulletin of Ecology and Environment of the People's Republic of China
978 2019. , [http://www.mee.gov.cn/hjzl/sthjzk/zghjzkgb/202006/P02020060250946](http://www.mee.gov.cn/hjzl/sthjzk/zghjzkgb/202006/P020200602509464172096.pdf)
979 [4172096.pdf](http://www.mee.gov.cn/hjzl/sthjzk/zghjzkgb/202006/P020200602509464172096.pdf), 2020 (last access: 31 October 2021).

980 MEE (Ministry of Ecology and Environment of the People's Republic of China):
981 Bulletin of Ecology and Environment of the People's Republic of China 2020.,
982 2021 (last access: 31 October 2021).

983 Mook, W., and Johannes, V.: Reporting 14C Activities and Concentrations,
984 Radiocarbon, 41, 227-239, <https://doi.org/10.1017/S0033822200057106>, 1999.

985 Moura, J., Martens, C., Moreira, M., Lima, R., and Menton, M.: Spatial and seasonal
986 variations in the stable carbon isotopic composition of methane in stream
987 sediments of eastern Amazonia, Tellus B, 60, 21-31,
988 <https://doi.org/10.1111/j.1600-0889.2007.00322.x>, 2008.

989 NBS: (National bureau of statistics): China Statistical Yearbook-2019. , China
990 Statistics press. , <http://www.stats.gov.cn/tjsj/ndsj/2019/indexch.htm>, 2020 (last
991 access: 31 October 2021).

992 NBS (National bureau of statistics): China Statistical Yearbook-2020., China Statistics
993 press. , <http://www.stats.gov.cn/tjsj/ndsj/2020/indexch.htm>, 2021 (last access: 31



- 994 October 2021).
- 995 Ni, H., Huang, R., Cao, J., Liu, W., Zhang, T., Wang, M., Meijer, H., and Dusek, U.:
- 996 Source apportionment of carbonaceous aerosols in Xi'an, China: insights from a
- 997 full year of measurements of radiocarbon and the stable isotope C-13,
- 998 Atmospheric Chemistry & Physics, <https://doi.org/10.5194/acp-18-16363-2018>,
- 999 2018.
- 1000 Ni, H., Huang, R., Cosijn, M., Yang, L., and Dusek, U.: Measurement report:
- 1001 dual-carbon isotopic characterization of carbonaceous aerosol reveals different
- 1002 primary and secondary sources in Beijing and Xi'an during severe haze events,
- 1003 Atmospheric Chemistry & Physics, 20, 16041-16053,
- 1004 <https://doi.org/10.5194/acp-20-16041-2020>, 2020.
- 1005 Niu, Z., Wang, S., Chen, J., Zhang, F., Chen, X., He, C., Lin, L., Yin, L., and Xu, L.:
- 1006 Source contributions to carbonaceous species in PM_{2.5} and their uncertainty
- 1007 analysis at typical urban, peri-urban and background sites in southeast China,
- 1008 Environmental Pollution, 181, 107-114,
- 1009 <https://doi.org/10.1016/j.envpol.2013.06.006>, 2013.
- 1010 Niu, Z., Zhou, W., Peng, C., Wu, S., Lu, X., Xiong, X., Hua, D., and Fu, Y.:
- 1011 Observations of Atmospheric $\Delta^{14}\text{C}_{\text{CO}_2}$ at the Global and Regional
- 1012 Background Sites in China: Implication for Fossil Fuel CO_2 Inputs,
- 1013 Environmental Science & Technology, 50, 12122-12128, 2016.
- 1014 Niu, Z., Feng, X., Zhou, W., Wang, P., Liu, Y., Lu, X., Du, H., Fu, Y., Li, M., Mei, R.,
- 1015 Li, Q., and Cai, Q.: Tree-ring $\Delta^{14}\text{C}$ time series from 1948 to 2018 at a regional
- 1016 background site, China: Influences of atmospheric nuclear weapons tests and
- 1017 fossil fuel emissions, Atmospheric Environment, 246,
- 1018 <https://doi.org/10.1016/j.atmosenv.2020.118156>, 2021.



- 1019 Novakov, T., Menon, S., Kirchstetter, T., Koch, D., and Hansen, J.: Aerosol organic
1020 carbon to black carbon ratios: Analysis of published data and implications for
1021 climate forcing, *Journal of Geophysical Research Atmospheres*, 110,
1022 <https://doi.org/10.1029/2005JD005977>, 2005.
- 1023 Oros, D., and Simoneit, B.: Identification and emission factors of molecular tracers in
1024 organic aerosols from biomass burning Part 1. Temperate climate conifers,
1025 *Applied Geochemistry*, 16, 1513-1544,
1026 [https://doi.org/10.1016/s0883-2927\(01\)00021-x](https://doi.org/10.1016/s0883-2927(01)00021-x), 2001a.
- 1027 Oros, D., and Simoneit, B.: Identification and emission factors of molecular tracers in
1028 organic aerosols from biomass burning Part 2. Deciduous trees, *Applied*
1029 *Geochemistry*, 16, 1545-1565, [https://doi.org/10.1016/s0883-2927\(01\)00022-1](https://doi.org/10.1016/s0883-2927(01)00022-1),
1030 2001b.
- 1031 PGHP: (The People's Government of Hebei Province): Hebei Economic
1032 Yearbook-2020, China Statistics press, 2021 (last access: 31 October 2021).
- 1033 Puxbaum, H., Caseiro, A., Sánchez-Ochoa, A., Kasper-Giebl, A., Claeys, M.,
1034 Gelencsér, A., Legrand, M., Preunkert, S., and Pio, C.: Levoglucosan levels at
1035 background sites in Europe for assessing the impact of biomass combustion on
1036 the European aerosol background, *Journal of Geophysical Research*, 112,
1037 D23S05, <https://doi.org/10.1029/2006jd008114>, 2007.
- 1038 SAPBS (Shaanxi Provincial Bureau of Statistics): Shaanxi Statistical Yearbook-2020,
1039 China Statistics press, <http://tjj.shaanxi.gov.cn/upload/n2020/indexch.htm>, 2020
1040 (last access: 31 October 2021).
- 1041 Seinfeld, J., and Pandis, S.: *Atmospheric Chemistry and Physics: From Air Pollution*
1042 *to Climate Change, Environment ence & Policy for Sustainable Development*,
1043 1998.



- 1044 Shang, J., Khuzestani, R., Tian, J., Schauer, J., Hua, J., Zhang, Y., Cai, T., Fang, D.,
1045 An, J., and Zhang, Y.: Chemical characterization and source apportionment of
1046 PM_{2.5} personal exposure of two cohorts living in urban and suburban Beijing,
1047 Environmental Pollution, <https://doi.org/10.1016/j.envpol.2018.11.076>, 2019.
- 1048 Shao, M., Li, J., and Tang, X.: The application of accelerator mass spectrometry
1049 (AMS) in the study of source identification of aerosols (in Chinese). Acta
1050 Scientiae Circumstantiae 16 (2), 130–141, 1996.
- 1051 Shen, G., Wei, W., Yang, Y., Chen, Z., Min, Y., Miao, X., Ding, J., Wei, L., Wang, B.,
1052 and Shen, H.: Emission factors and particulate matter size distribution of
1053 polycyclic aromatic hydrocarbons from residential coal combustions in rural
1054 Northern China, Atmospheric Environment, 44, 5237-5243,
1055 <https://doi.org/10.1016/j.atmosenv.2010.08.042>, 2010.
- 1056 Shen, Z., Cao, J., Liu, S., Zhu, C., Wang, X., Zhang, T., Xu, H., and Hu, T.: Chemical
1057 Composition of PM₁₀ and PM_{2.5} Collected at Ground Level and 100 Meters
1058 during a Strong Winter-Time Pollution Episode in Xi'an, China, Journal of the
1059 Air & Waste Management Association,
1060 <https://doi.org/10.1080/10473289.2011.608619>, 2011.
- 1061 Simoneit, B., Schauer, J., Nolte, C., Oros, D., Elias, V., Fraser, M., Rogge, W., and
1062 Cass, G.: Levoglucosan, a tracer for cellulose in biomass burning and
1063 atmospheric particles, Atmospheric Environment, 33, 173-182,
1064 [https://doi.org/10.1016/S1352-2310\(98\)00145-9](https://doi.org/10.1016/S1352-2310(98)00145-9), 1999.
- 1065 Simpson, D., Yttri, K. E., Klimont, Z., Kupiainen, K., Caseiro, A., Gelencsér, A., Pio,
1066 C., Puxbaum, H., and Legrand, M.: Modeling carbonaceous aerosol over Europe:
1067 Analysis of the CARBOSOL and EMEP EC/OC campaigns, Journal of
1068 Geophysical Research Atmospheres, 112, -,



- 1069 <https://doi.org/10.1029/2006JD008158>, 2007.
- 1070 Slota, P., Jull, A., Linick, T., and Toolin, L.: Preparation of Small Samples for ^{14}C
1071 Accelerator Targets by Catalytic Reduction of CO , *Radiocarbon*, 29, 303-306,
1072 <https://doi.org/10.1017/S0033822200056988>, 1987.
- 1073 Smith, B., and Epstein, S.: Two Categories of $^{13}\text{C}/^{12}\text{C}$ Ratios for Higher Plants, *Plant*
1074 *physiology*, 47, 380-384, <https://doi.org/10.1029/2006JD008158>, 1971.
- 1075 Song, Y., Zhang, Y., Xie, S., Zeng, L., Zheng, M., Salmon, L., Shao, M., and Slanina,
1076 S.: Source apportionment of $\text{PM}_{2.5}$ in Beijing by positive matrix factorization,
1077 *Atmospheric Environment*, 40, 1526-1537,
1078 <https://doi.org/10.1016/j.atmosenv.2005.10.039>, 2006.
- 1079 SPBS (Shanxi Provincial Bureau of Statistics): *Shanxi Statistical Yearbook-2019*,
1080 *China Statistics*
1081 press, <http://tjj.shaanxi.gov.cn/upload/2020/pro/3sxtjnj/zk/indexch.htm>, 2020
1082 (last access: 31 October 2021).
- 1083 Streets, D., Bond, T., Carmichael, G., Fernandes, S., Fu, Q., He, D., Klimont, Z.,
1084 Nelson, S., Tsai, N., Wang, M., Woo, J., and Yarber, K.: An inventory of gaseous
1085 and primary aerosol emissions in Asia in the year 2000, *Journal of Geophysical*
1086 *Research: Atmospheres*, 108, <https://doi.org/10.1029/2002JD003093>, 2003.
- 1087 Stuiver, M., and Polach, H.: Discussion: Reporting of ^{14}C data, 1977.
- 1088 Sun, X., Hu, M., Guo, S., Liu, K., and Zhou, L.: ^{14}C -Based source assessment of
1089 carbonaceous aerosols at a rural site, *Atmospheric Environment*, 50, 36-40,
1090 <https://doi.org/10.1016/j.atmosenv.2012.01.008>, 2012.
- 1091 Szidat, S., Jenk, T., Gaeggeler, H., Synal, H., Hajdas, I., Bonani, G., and Saurer, M.:
1092 THEODORE, a two-step heating system for the EC/OC determination of
1093 radiocarbon (^{14}C) in the environment, *Nuclear Instruments and Methods in*



- 1094 Physics Research Section B Beam Interactions with Materials and Atoms, 223,
1095 829-836, <https://doi.org/10.1016/j.nimb.2004.04.153>, 2004.
- 1096 Szidat, S., Jenk, T., Synal, H., Kalberer, M., Wacker, L., Hajdas, I., Kasper-Giebl, A.,
1097 and Baltensperger, U.: Contributions of fossil fuel, biomass burning, and
1098 biogenic emissions to carbonaceous aerosols in Zürich as traced by ^{14}C , Journal
1099 of Geophysical Research Atmospheres, 111,
1100 -, <http://doi.org/10.1029/2005JD006590>, 2006.
- 1101 Szidat, S., Ruff, M., Perron, N., Wacker, L., Synal, H. A., Hallquist, M., Shannigrahi,
1102 A. S., Yttri, K., Dye, C., and Simpson, D.: Fossil and non-fossil sources of
1103 organic carbon (OC) and elemental carbon (EC) in Göteborg, Sweden,
1104 Atmospheric Chemistry & Physics, 9, 16255-16289,
1105 <https://doi.org/10.5194/acpd-8-16255-2008>, 2009.
- 1106 Tanarit, S., Alex, G., Detlev, H., Jana, M., and Christine, W.: Secondary Organic
1107 Aerosol from Sesquiterpene and Monoterpene Emissions in the United States,
1108 Environmental Science & Technology, 42, 8784–8790,
1109 <https://doi.org/10.1021/es800817r>, 2008.
- 1110 Tian, S., Pan, Y., and Wang, Y.: Size-resolved source apportionment of particulate
1111 matter in urban Beijing during haze and non-haze episodes, Atmospheric
1112 Chemistry & Physics, 16, 9405-9443, <https://doi.org/10.5194/acp-16-1-2016>,
1113 2016.
- 1114 Turekian, V., Macko, S., Ballentine, D., Swap, R., and Garstang, M.: Causes of bulk
1115 carbon and nitrogen isotopic fractionations in the products of vegetation burns:
1116 laboratory studies, Chemical Geology, 152, 181-192, 1998.
- 1117 Turnbull, J. C., Lehman, S. J., Miller, J. B., Sparks, R. J., Southon, J. R., and Pieter P.
1118 Tans: A new high precision ^{14}C time series for North American continental air,



- 1119 Journal of Geophysical Research, <http://doi.org/10.1029/2006jd008184>, 2007.
- 1120 Turpin, B., and Huntzicker, J.: Identification of secondary organic aerosol episodes
1121 and quantitation of primary and secondary organic aerosol concentrations during
1122 SCAQS, Atmospheric Environment, 29, 3527-3544,
1123 [https://doi.org/10.1016/1352-2310\(94\)00276-Q](https://doi.org/10.1016/1352-2310(94)00276-Q), 1995.
- 1124 Vonwiller, M., Quintero, G., and Szidat, S.: Isolation and ¹⁴C analysis of humic-like
1125 substances (HULIS) from ambient aerosol samples, 2017.
- 1126 Wang, G., Kawamura, K., Cheng, C., Li, J., Cao, J., Zhang, R., Zhang, T., Liu, S., and
1127 Zhao, Z.: Molecular distribution and stable carbon isotopic composition of
1128 dicarboxylic acids, ketocarboxylic acids, and α -dicarbonyls in size-resolved
1129 atmospheric particles from Xi'an City, China, Environmental Science &
1130 Technology, 46, 4783-4791, <https://doi.org/10.1021/es204322c>, 2012.
- 1131 Wang, G., Cheng, S., Li, J., Lang, J., Wen, W., Yang, X., and Tian, L.: Source
1132 apportionment and seasonal variation of PM_{2.5} carbonaceous aerosol in the
1133 Beijing-Tianjin-Hebei Region of China, Environmental Monitoring and
1134 Assessment, 187, 1-13, <https://doi.org/10.1007/s10661-015-4288-x>, 2015.
- 1135 Wang, H., Zhuang, Y., Wang, Y., Yuan, Y., and Zhuang, G.: Long-term monitoring and
1136 source apportionment of PM_{2.5}/PM₁₀ in Beijing, China, Journal of
1137 Environmental Sciences, 20, 1323-1327,
1138 [https://doi.org/10.1016/S1001-0742\(08\)62228-7](https://doi.org/10.1016/S1001-0742(08)62228-7), 2008.
- 1139 Wang, Z., Bi, X., Sheng, G., and Fu, J.: Characterization of organic compounds and
1140 molecular tracers from biomass burning smoke in South China I: Broad-leaf trees
1141 and shrubs, Atmospheric Environment, 43, 3096-3102,
1142 <https://doi.org/10.1016/j.atmosenv.2009.03.012>, 2009.
- 1143 Weber, R., Sullivan, A., Peltier, R., Russell, A., Yan, B., Zheng, M., Gouw, J. D.,



- 1144 Warneke, C., Brock, C., and Holloway, J.: A study of secondary organic aerosol
1145 formation in the anthropogenic-influenced southeastern United States, *Journal of*
1146 *Geophysical Research Atmospheres*, 112, D13302,
1147 <https://doi.org/10.1029/2007jd008408>, 2007.
- 1148 Widory, D., Roy, S., Moullec, Y., Goupil, G., Cocherie, A., and Guerrot, C.: The
1149 origin of atmospheric particles in Paris: a view through carbon and lead isotopes,
1150 *Atmospheric Environment*, 38, 953-961,
1151 <https://doi.org/10.1016/j.atmosenv.2003.11.001>, 2004.
- 1152 Widory, D.: Combustibles, fuels and their combustion products: A view through
1153 carbon isotopes, *Combustion Theory & Modelling*, 10, 831-841,
1154 <https://doi.org/10.1080/13647830600720264>, 2006.
- 1155 Winiger, P., Andersson, A., Eckhardt, S., Stohl, A., Semiletov, I., Dudarev, O., Charkin,
1156 A., Shakhova, N., Klimont, Z., and Heyes, C.: Siberian Arctic black carbon
1157 sources constrained by model and observation, *Proc Natl Acad Sci U S A*, 114,
1158 E1054, <https://doi.org/10.1073/pnas.1613401114>, 2017.
- 1159 XAMBS (Xi'an Municipal Bureau Statistics): Xi'an Statistical Yearbook-2020 China
1160 Statistics press, <http://tjj.xa.gov.cn/tjnj/2020/zk/indexch.htm>, 2021 (last access:
1161 31 October 2021).
- 1162 Yan, X., and Crookes, R.: Energy demand and emissions from road transportation
1163 vehicles in China, *Progress in Energy & Combustion Science*, 36, 651-676,
1164 <https://doi.org/10.1016/j.pecs.2010.02.003>, 2010.
- 1165 Yang, F., He, K., Ye, B., Chen, X., Cha, L., Cadle, S., Chan, T., and Mulawa, P.:
1166 One-year record of organic and elemental carbon in fine particles in downtown
1167 Beijing and Shanghai, *Atmospheric Chemistry & Physics*, 5, 1449-1457,
1168 <https://doi.org/10.5194/acp-5-1449-2005>, 2005.



- 1169 Yttri, K., Simpson, D., Nøjgaard, J., Kristensen, K., Genberg, J., Stenstr, M.,
1170 Swietlicki, E., Hillamo, R., Aurela, M., Bauer, H., JH., O., M, J., C, D., S, E., JF,
1171 B., A, S., and Glasius, M.: Source apportionment of the summer time
1172 carbonaceous aerosol at Nordic rural background sites, Atmospheric Chemistry
1173 & Physics Discussions, 11, 13339-13357,
1174 <https://doi.org/10.5194/acpd-11-16369-2011>, 2011.
- 1175 Zhang, R., Jing, J., Tao, J., Hsu, S., Wang, G., Cao, J., Lee, C., Zhu, L., Chen, Z., and
1176 Zhao, Y.: Chemical characterization and source apportionment of PM_{2.5} in
1177 Beijing: seasonal perspective, Atmospheric Chemistry & Physics, 13, 7053-7074,
1178 <https://doi.org/10.5194/acp-14-175-2014>, 2014.
- 1179 Zhang, Y., Shao, M., Zhang, Y., Zeng, L., LingYan, H., Zhu, B., Wei, Y., and Zhu, X.:
1180 Source profiles of particulate organic matters emitted from cereal straw burnings,
1181 Journal of Environmental Sciences, 19, 167-175,
1182 [https://doi.org/10.1016/S1001-0742\(07\)60027-8](https://doi.org/10.1016/S1001-0742(07)60027-8), 2007.
- 1183 Zhang, Y., Perron, N., Ciobanu, V., Zotter, P., and Szidat, S.: On the isolation of OC
1184 and EC and the optimal strategy of radiocarbon-based source apportionment of
1185 carbonaceous aerosols, Soil Biology & Biochemistry, 12, 17657-17702,
1186 <https://doi.org/10.5194/acpd-12-17657-2012>, 2012.
- 1187 Zhang, Y., Huang, R., Haddad, I., Ho, K., Cao, J., Han, Y., Zotter, P., Bozzetti, C.,
1188 Daellenbach, K. R., Canonaco, F., Slowik, J., Salazar, G., Schwikowski, M.,
1189 Schnelle-Kreis, J., Abbaszade, G., Zimmermann, R., Baltensperger, U., Prévôt, A.
1190 S. H., and Szidat, S.: Fossil vs. non-fossil sources of fine carbonaceous aerosols
1191 in four Chinese cities during the extreme winter haze episode of 2013,
1192 Atmospheric Chemistry & Physics, 15, 1299-1312,
1193 <https://doi.org/10.5194/acp-15-1299-2015>, 2015.



- 1194 Zhang, Y., Ren, H., Sun, Y., Cao, F., Chang, Y., Liu, S., Lee, X., Agrios, K.,
1195 Kawamura, K., Liu, D., Ren, L., Du, W., Wang, Z., Prévôt, A. S. H., Szidat, S.,
1196 and Fu, P.: High Contribution of Nonfossil Sources to Submicrometer Organic
1197 Aerosols in Beijing, China, *Environmental Science & Technology*, 51, 7842,
1198 <https://doi.org/10.1021/acs.est.7b01517>, 2017.
- 1199 Zhang, Z., Engling, G., Chan, C., Yang, Y., Lin, M., Shi, S., He, J., Li, Y., and Wang,
1200 X.: Determination of isoprene-derived secondary organic aerosol tracers
1201 (2-methyltetrols) by HPAEC-PAD: Results from size-resolved aerosols in a
1202 tropical rainforest, *Atmospheric Environment*, 70, 468-476,
1203 <https://doi.org/10.1016/j.atmosenv.2013.01.020>, 2013.
- 1204 Zhao, P., Fan, D., Yang, Y., Di, H., and Liu, H.: Characteristics of carbonaceous
1205 aerosol in the region of Beijing, Tianjin, and Hebei, China, *Atmospheric*
1206 *Environment*, 71, 389–398, <https://doi.org/10.1016/j.atmosenv.2013.02.010>,
1207 2013.
- 1208 Zhi, G., Chen, Y., Feng, Y., Xiong, S., Jun, L., Zhang, G., Sheng, G., and Jiamo, F.:
1209 Emission characteristics of carbonaceous particles from various residential
1210 coal-stoves in China, *Environmental Science & Technology*, 42, 3310,
1211 <https://doi.org/10.1021/es702247q>, 2008.
- 1212 Zhou, W., Zhao, X., Xuefeng, L., Lin, L., Zhengkun, W., Peng, C., Wengnian, Z., and
1213 Chunhai, H.: The 3MV multi-element AMS in Xi'an, China: Unique features and
1214 preliminary tests, *Radiocarbon*, 48, 285-293,
1215 <https://doi.org/10.1016/j.atmosenv.2014.05.058>, 2006.
- 1216 Zhou, W., Lu, X., Wu, Z., Zhao, W., Huang, C., Li, L., Peng, C., and Xin, Z.: New
1217 results on Xi'an-AMS and sample preparation systems at Xi'an-AMS center,
1218 *Nuclear Instruments & Methods in Physics Research*, 262, 135-142,



- 1219 <https://doi.org/10.1016/j.nimb.2007.04.221>, 2007.
- 1220 Zhou, W., Wu, S., Huo, W., Xiong, X., Cheng, P., Lu, X., and Niu, Z.: Tracing fossil
- 1221 fuel CO₂ using $\Delta^{14}\text{C}$ in Xi'an City, China, Atmospheric Environment, 94,
- 1222 538-545, <https://doi.org/10.1017/S0033822200066492>, 2014.
- 1223